CHAPTER 5B
ELEMENTS OF DYNAMICAL OCEANOGRAPHY

In the previous chapter we derived the following the continuity and conservation of momentum equations that are pertinent to the ocean, namely

$$\frac{\partial u}{\partial x}+\frac{\partial v}{\partial y}+\frac{\partial w}{\partial z}=0 \qquad \text{Continuity}$$

and he vector form of Newton's 2nd Law per unit volume for a fluid ocean

$$\rho\frac{d\vec{V}}{dt}=\rho\left(\frac{\partial\vec{V}}{\partial t}+(\vec{V}\bullet\nabla)\vec{V}\right)=-\rho(2\vec{\Omega}\times\vec{V})-\nabla p-\rho g\vec{k}+\vec{F}^{f} \qquad \text{Momentum}$$

The component form of the momentum equation, in which we have neglected the less important Coriolis terms, is

$$\frac{du}{dt}=fv-\frac{1}{\rho}\frac{\partial p}{\partial x}+F_x^f$$

$$\frac{dv}{dt}=-fu-\frac{1}{\rho}\frac{\partial p}{\partial y}+F_y^f$$

$$\frac{dw}{dt}=-\frac{1}{\rho}\frac{\partial p}{\partial z}-g+F_z^f$$

where $F_x^f=\left(\frac{\partial\tau_{zx}}{\partial z}+\left[\frac{\partial\tau_{yx}}{\partial y}\right]\right)$; $F_y^f=\left(\frac{\partial\tau_{zy}}{\partial z}+\left[\frac{\partial\tau_{xy}}{\partial x}\right]\right)$ $F_z^f=\left(\frac{\partial\tau_{yz}}{\partial y}+\left[\frac{\partial\tau_{xz}}{\partial x}\right]\right)$

Now let's consider approximations of the above set of equations that yield the essential physics of a suite of ocean processes of interest. The first approximation is to *assume no flow acceleration*. To assume a steady flow, i.e.

$$\frac{\partial}{\partial t}\equiv 0\ ,$$

where ≡ means "defined", eliminates time-dependent accelerations. Hence there is no

pulsing of the flow. However convective accelerations of the steady flow $(\overline{V} \bullet \nabla)\overline{V}$ are still possible. In many oceanic situations, these terms are small and can be neglected when compared to other terms in the equations. Thus for the following set of considerations, we will assume that $(\vec{V} \bullet \nabla)\vec{V} \gg 1$ and $\frac{\partial \vec{v}}{\partial t} \equiv 0$ so that we have <u>equilibrium</u> flows in which

$$\frac{d}{dt} \equiv 0 \ .$$

Therefore the component form of the momentum equations can be written as

$$\frac{1}{r}\frac{\partial p}{\partial x} = fv + F_x^r$$
$$\frac{1}{r}\frac{\partial p}{\partial y} = -fu + F_y^r$$
$$\frac{1}{r}\frac{\partial p}{\partial z} = -g + F_z^r$$

If we further assume that friction forces are negligible, then

$$\frac{1}{r}\frac{\partial p}{\partial x} = fv$$
$$\frac{1}{r}\frac{\partial p}{\partial y} = -fu$$
$$\frac{1}{r}\frac{\partial p}{\partial z} = -g$$

Hydrostatic Balance

Recall that if we assume static conditions or <u>no motion</u> (i.e., $\vec{V} \equiv 0$), then the above three equations reduce to the *hydrostatic balance* – the *force balance* between the pressure gradient force and the water parcel weight per unit volume according to

$$\frac{\partial p}{\partial z} = - r\, g\,.$$

We explored the implications of a hydrostatic ocean pressure field above, so that we will move on and consider the force balance that leads to horizontal geostrophic flow in the presence of an approximate or quasi- hydrostatic ocean.

Geostrophic Balance

One of the simpler force balances is between the pressure gradient and Coriolis forces CF, which is illustrated in (Figure 5.21).

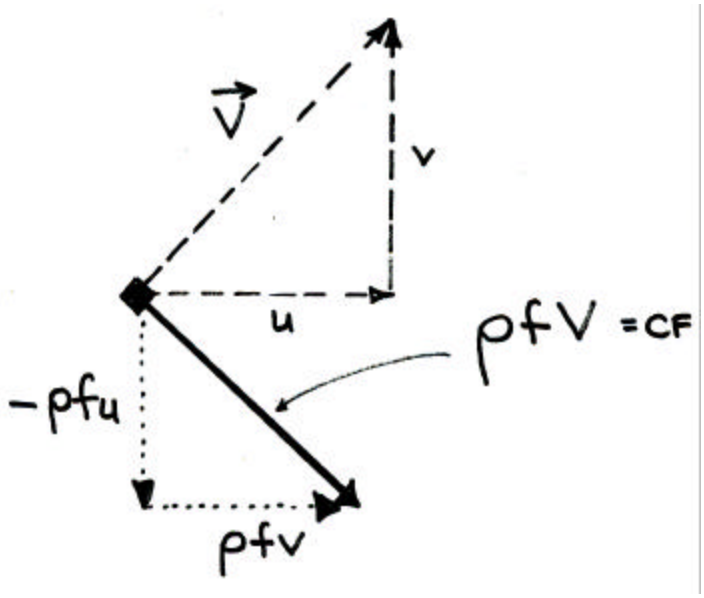

Figure 5.21 The generalized Coriolis force (CF) on a water parcel with a speed V.

The *geostrophic force balance* in Cartesian component form is

$$r\,\mathrm{fv} - \frac{\partial p}{\partial x} = 0$$

$$- r\,\mathrm{fu} - \frac{\partial p}{\partial y} = 0$$

and leads to a condition known as *geostrophic flow*.

The generalized form of the geostrophic balance, in a coordinate system aligned with the

water parcel flow vector, can be derived by squaring and summing the Cartesian components so that

$$r^2 f^2 (v^2 + u^2) = \frac{\partial p^2}{\partial x} + \frac{\partial p^2}{\partial y} \qquad \text{or} \qquad r\, f\, |\vec{V}| = \frac{\partial p}{\partial n} \quad ,$$

where $|\vec{V}|$ is the magnitude of the total velocity and *n* is the coordinate perpendicular to $\vec{V}$ with the sense shown in Figure 5.22a.

Thus, in general, the pressure gradient force (PGF) and Coriolis force (CF) are balanced in the direction perpendicular to the flow vector... *no matter* what its direction (Figure 5.22b). Because the Coriolis parameter *f* is of the opposite sign in the northern and southern hemisphere, the Coriolis force is to the left of the velocity direction in the southern hemisphere.

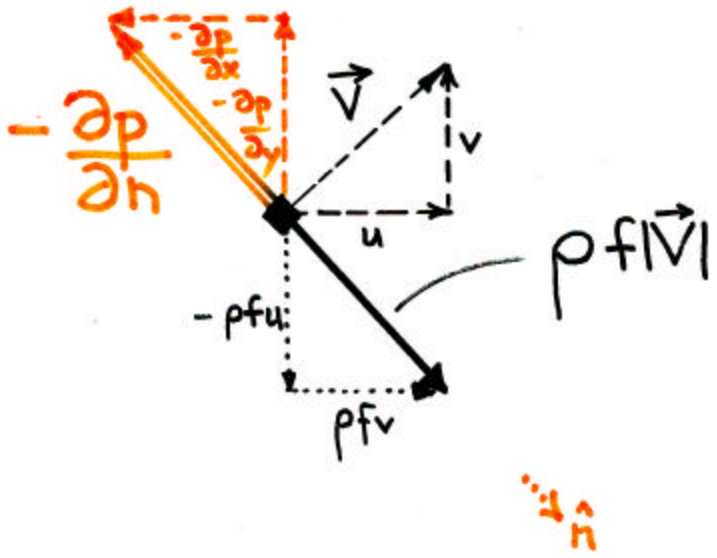

Figure 5.22a Generalized geostrophic force balance for a water parcel. The Coriolis force $r\ f\ V$ balances the pressure gradient force $-dp/dn$ in the direction normal to the velocity $\vec{V} = u\vec{i} + v\vec{j}$. The Cartesian components of the velocity and pressure gradient are also shown.

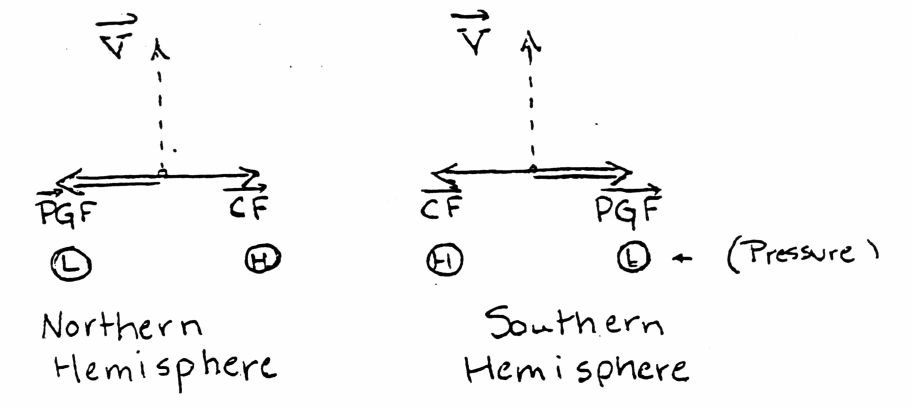

Figure 5.22b Comparison of the generalized geostrophic force balances relative to the flow velocity vector in the northern and southern hemisphere respectively. Note generalized pressure distribution.

Note that this geometry of the geostrophic flow situation ensures that the Coriolis force can never *do any work* on the water parcel (i.e. $\vec{CF} \bullet \vec{V} = 0$) and therefore *can not initiate motion* (i.e. change the kinetic energy)! This realization is consistent with the fact that the Coriolis "force" is a pseudo force, (i.e., really only an acceleration). Thus the flow $\vec{V}$ must have been initiated by some other physical process like wind forcing – a process that we will explore later. However, once the water is moving for more than about a half day, the geostrophic relation above specifies the magnitude of the pressure gradient force *required* to maintain the force balance. Because geostrophic flow is strictly un-accelerated by assumption,, the curvature effects (or $\frac{r\,V^2}{r}$) associated with the flow must be small compared to Coriolis effects $r\,fV$. Thus strictly speaking geostrophic flow is horizontal straight-line or *rectilinear* ocean flow.

Let's explore the relation between the pressure field and the geostrophic flow. First of all, the hydrostatic condition of no flow and level isobaric surfaces is replaced by geostrophic flow and isobaric surfaces that are tilted relative to geopotential surfaces. How much tilt? To determine this, consider the picture in Figure 5.23, in which ß is positive counterclockwise. The finite-difference form of the hydrostatic relation tells us that pressure difference $d\,p$ over a distance $d\,n$ is $d\,p = g\,r\,dz$. Substituting this relation into the finite difference form of the geostrophic relation

$$\frac{d\,\mathrm{p}}{d\,\mathrm{n}} = r\,\mathrm{fV}$$

and rearranging gives

$$\frac{d\,\mathrm{z}}{d\,\mathrm{n}} = \frac{\mathrm{fV}}{\mathrm{g}}.$$

Since tanß = dz/dn, the relation for the tilt of the isobaric surface is

$$\tan b = \mathrm{fV/g}\,. \qquad ,$$

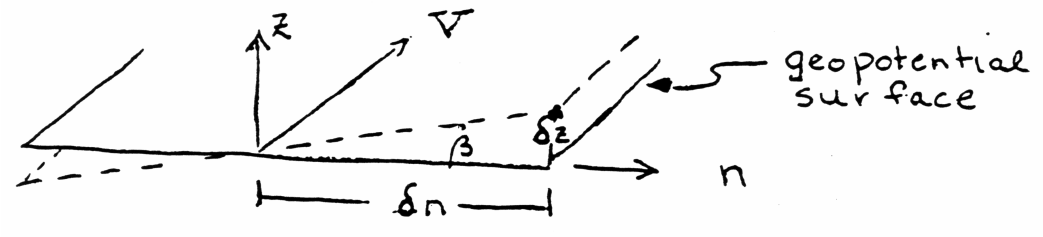

Figure 5.23 Schematic of geostrophic flow on an isobaric surface tilted an angle ß relative to a geopotential surface.

So given a geostrophic flow velocity, the isobaric tilt can be computed; (Note that ß > 0 in the northern hemisphere). But what are the typical values of ß? To estimate this, consider the tilt of the sea surface which is nearly an isobaric surface: Assuming that f ~ 10^{-4} rad/sec, g ~10^{3} cm/sec^{2}, and V ~ 100 cm/sec yields $\tan b = 10^{-5}$ or a slope of 1 cm/km. Thus we find that, although isobaric surfaces are not exactly level, they are nearly so and because of that the hydrostatic condition is *almost* exact.

Now assume the isobaric surface above is the ocean surface. If the water column below the surface is homogeneous (i.e. s_q = constant), then density r is a function of pressure alone (i.e. $r = r(p)$). Under this circumstance the isobars and isopycnals are parallel (Figure 5.24).

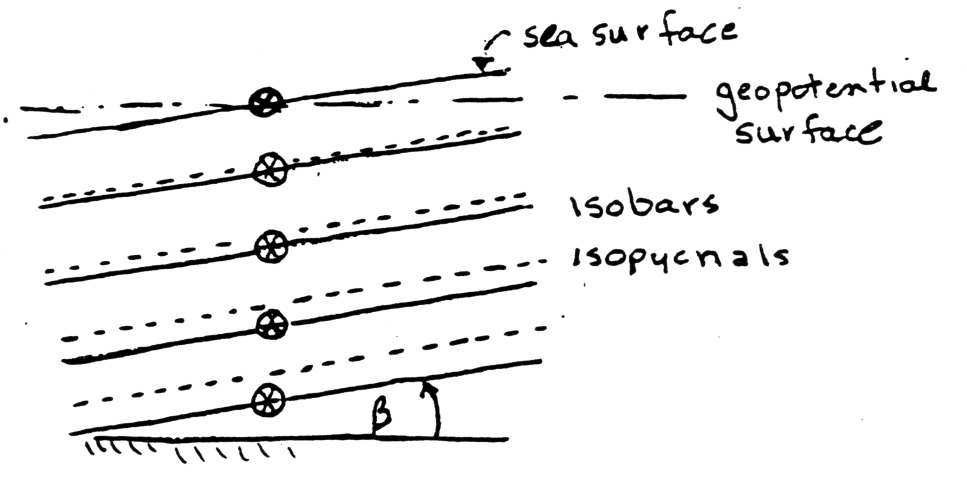

Figure 5.24 The configuration of isobars and isopycnals in a homogeneous ocean geostrophic flow.

Therefore, since $V = \frac{g}{f} \tan b$ everywhere, the geostrophic flow velocity V is *depth-independent. Depth-independent flow structure is called barotropic flow*. This is specific example of geostrophic *barotropic flow*.

However in general in the ocean, potential density (or s_q) is not constant. Therefore $p \neq r(p)$ and isobars and isopycnals are generally not parallel. Nevertheless, at each isobar $V = \frac{g}{f} \tan b$. However, since isobar tilts vary with depth [i.e. ß = ß(z)], V = V(z) and we have a geostrophic flow example of a *depth-dependent flow* that is generally called *baroclinic flow*.

How is the change of velocity with depth or velocity shear, $\frac{\partial V}{\partial z}$ related to the density field? Consider a two layer system (Figure 5.25) in which the surface is level and the interface between the upper layer (with $r = r_1$) and lower layer (with $r = r_2 > r_1$) is inclined at angle ß.

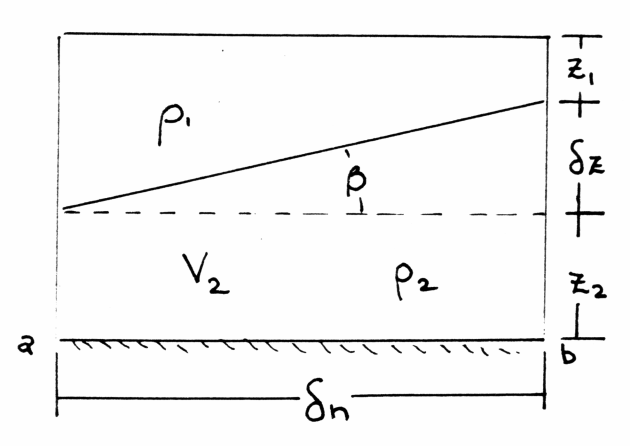

Figure 5.25 A two layer ocean with reclined interface.

There is no horizontal PG in upper layer for $z > z_1$! However in the lower layer, the lateral pressure gradient is

$$\frac{d\,p}{d\,n} = \frac{p_b - p_a}{d\,n} = \frac{g}{d\,n}[\rho_2(d_z + z_2) + \rho_1 z_1) - (\rho_2 z_2 + \rho_1(z_1 + d\,z)]$$

$$= \frac{g}{d\,n}(\rho_2 - d_1)\,d_z$$

$$\frac{d\,p}{d\,n} = g(\rho_2 - \rho_1)\frac{\partial z}{\partial n}$$

Thus the geostrophic velocity in lower layer is

$$V_2 = \frac{g}{\rho_2 f}(\rho_2 - \rho_1)\tan\beta$$

Geostrophic Frontal Flow: The Margules Equation

Often the horizontal density gradients are relatively large, approximating a density discontinuity or "front". These are common in the atmosphere and the ocean as well. To explore such fronts, consider the model in Figure 5.26.

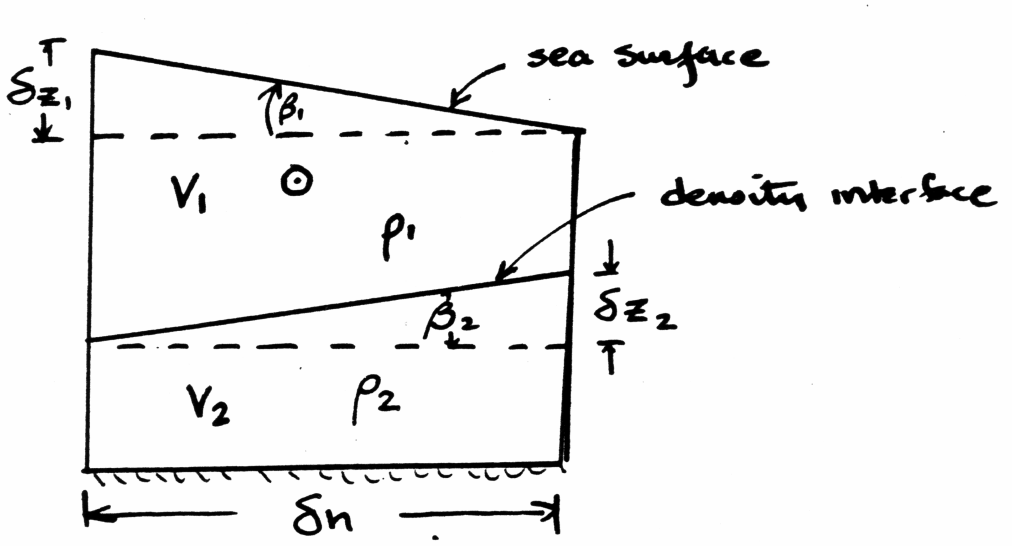

Figure 5.26. Configuration of a two-layer geostrophic flow system.

Your homework problem showed you that the lower layer pressure gradient in this situation is

$$\frac{d\,p^{l}}{d\,n} = g(\rho_2 - \rho_1)\frac{d\,z_2}{d\,n} - \rho_1 g\frac{d\,z_1}{d\,n}$$

Since the lower layer geostrophic flow (normal to the section) V_2 is $\frac{d\,p^{l}}{d\,n} = \rho_2 f V_2$

$$\rho_2 f V_2 = g(\rho_2 - \rho_1)\frac{d\,z_2}{d\,n} - \rho_1 g\frac{d\,z_1}{d\,n}$$

The upper layer pressure gradient and geostrophic flow is

$$\frac{d\,p^{u}}{d\,n} = -\rho_1 g\frac{d\,z_1}{d\,n} = \rho_1 f V_1 .$$

Combining the upper and lower layer relations from above leads to

$$\rho_2 f V_2 = g(\rho_2 - \rho_1)\frac{d\,z_2}{d\,n} + \rho_1 f V_1 \qquad ,$$

which can be rewritten in terms of the interface angle according to

$$\tan b_2 = \frac{f(r_2 V_2 - r_1 V_1)}{g(r_2 - r_1)} \qquad \text{Margules Equation}$$

Thus, if the right hand quantities are known, then the frontal slope can be calculated. Again assuming that f ~ 10^{-4} rad/sec, g ~10^3 cm/sec^2, and $V_1 = V_2$~ 100 cm/sec, it follows that

$$\tan b_2 = 10^{-7} \bullet \frac{10}{10^{-3}} = 10^{-3}$$

yields typical slopes for oceanic density interfaces of

$$\tan b_2 = 1 \text{ m per km}$$

and

$$\tan b_1 = 10^{-5} = 1 \text{ cm per km.}$$

Geostrophic Flow: Continuously Stratified Ocean

For a more general oceanic situation, consider the geostrophic flow in the smoothly-varying inhomogeneous ocean in Figure 5.27. (Note the similarity to Figure 5.26).

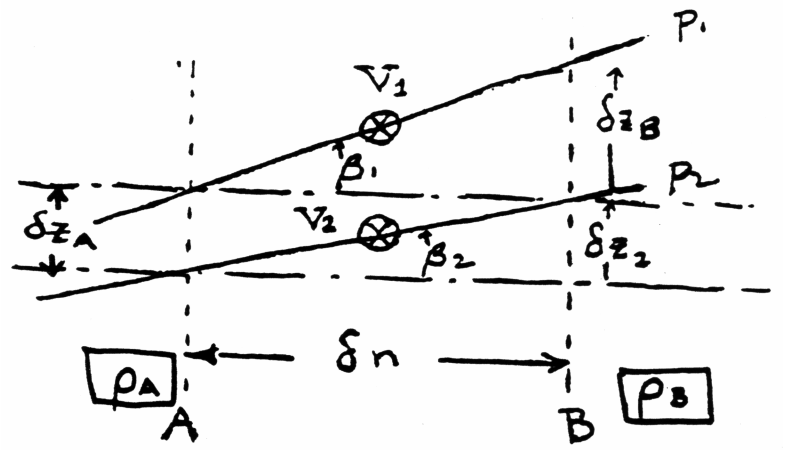

Figure 5.27 The geostrophic flow configuration of isobaric surfaces in an inhomogeneous fluid with r_B *is less than* r_A .

Given what we have already learned about computing the geostrophic flow velocity from the geometry of the isobars, compute the difference in the velocities ($dV = V_1 - V_2$) flowing along the p_1 and p_2 isobaric surfaces respectively according to

$$d\,\mathrm{V} = \frac{\mathrm{g}}{\mathrm{f}}(\tan \beta_1 - \tan \beta_2)$$

$$d\,V = \frac{\mathrm{g}}{\mathrm{f}}\left(\frac{d\,z_B - d\,z_A}{d\,\mathrm{n}}\right).$$

But the pressure difference between the two isobaric surfaces is always $p_2 - p_1$ and is related to the local water density via the hydrostatic relation;

$$p_2 - p_1 = \rho_A\, g\, d\,z_A = \rho_B\, g\, d\,z_B .$$

But because ρ_B *and* ρ_A are related by

$$\rho_B = \rho_A + \frac{d\,p}{d\,n} d\,n \qquad ,$$

our relation above becomes

$$\rho_A\, g\, d\,z_A = (\rho_A + \frac{\partial \rho}{\partial n} d\,n)\, g\, d\,z_B ,$$

which in turn can be reorganized as

$$\rho_A\, g(d\,z_B - d\,z_A) = -\,g\,\frac{\partial \rho}{\partial n} d\,n\, d\,z_B ,$$

Dividing through by ρ_A and substituting from above leads to the finite difference form for the velocity difference

$$d\,\mathrm{V} = -\,\frac{\mathrm{g}}{\rho_A\,\mathrm{f}}\,\frac{\partial \rho}{\partial n} d\,z_B .$$

For very small differences in the limit, the above relation becomes the more general differential relation

$$\frac{\partial V}{\partial z} = -\frac{g}{r f}\frac{\partial r}{\partial n}.$$

called the *Thermal Wind Relation* by the Scandinavian meteorologists around 1900. The thermal wind relation shows how the positive vertical shear in the velocity V is proportional to a negative density gradient normal to the velocity. Note in Figure 5.28 how the isopycnals and isobars intersect in this baroclinic flow case.

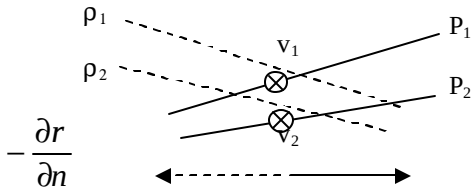

$-\frac{\partial r}{\partial n}$ density increases in negative direction

$+\frac{\partial p}{\partial n}$ pressure increases along a geopotenti al surface

Figure 5.28. The relationships of pressure and density fields in the thermal wind – an example of a baroclinic geostrophic flow field in which v1 > v2.

Computation of Geostrophic Velocities

As indicated earlier, the local partial differentials $\frac{\partial p}{\partial n}$ (or $\frac{\partial r}{\partial n}$ for that matter) can not be measured. However, the approximate geostrophic velocity vector can be computed from scalar pressure measurements using the finite difference form of the geostrophic

$$V = \frac{1}{r f}\frac{d p}{d n}$$

relation. In fact , this procedure is used by meteorologists to compute *geostrophic winds*. The surface pressure maps, which you see in the newspaper or on the nightly TV news, are usually a series of high and low pressure cells like those idealized in Figure 5.29.

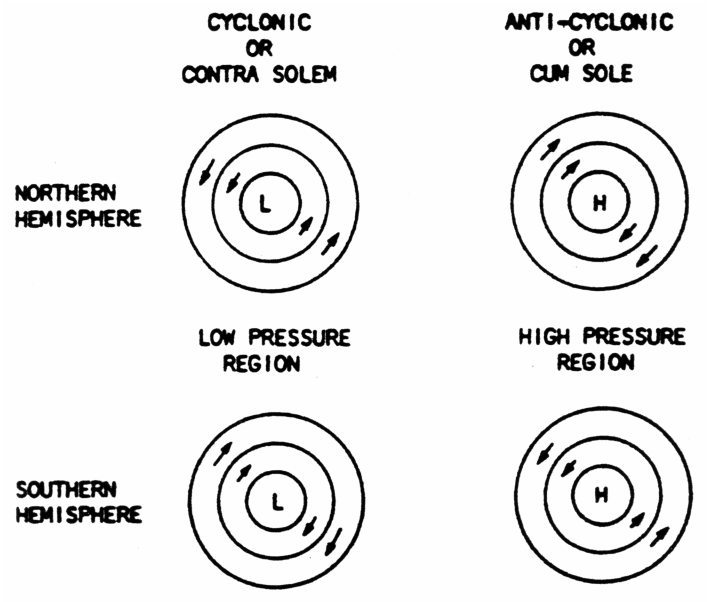

Figure 5.29. The sense of geostrophic winds associated with pressure "cells" composed of isobars.

Next the geostrophic and hydrostatic relations are used to explore the atmospheric pressure field. Assuming the following typical **atmospheric variable values**

$V \sim 10$ cm/sec

$\delta n \sim 10^3$ km $= 10^8$ cm

$\rho \sim 10^{-3}$ gm/cm^3

$f \sim 10^{-4}$ sec^{-1} (mid-latitude)

we estimate typical atmospheric pressure differences of $\delta p = V \rho f \delta n = 10^4$ dynes/cm^2. Since $p \sim 10^6$ dynes/cm^2 = 1 bar, the pressure difference to pressure ratio is

$$\frac{\delta p}{p}\Big|_{atmos} = 0.01 .$$

Since atmospheric pressures are relatively easy to measure accurately, they have been used for about a century to estimate geostrophic winds.

The situation in the ocean is very different, since typical ***oceanic variable values*** are:

$V \sim 10$ cm/sec

$d\ n \sim 100$ km $= 10^7$ cm

$r \sim 1$ gm/cm^3

Thus $d\ p = 10^4$ dynes/cm^2 , and $p = r\ gdh \sim 10^8$ dynes/cm^2 , and

$$d\ p/p\ |\text{ocean} = 0.0001 \quad ,$$

which is very small; making it very difficult to make direct pressure measurements that are accurate enough to infer geostrophic flow. Next we discuss how historically oceanographers have estimated geostrophic flow.

Method of Dynamic Sections

Oceanographers use a *modified form* of the "thermal wind" relation, with hydrographic station T and S data (Figure 5.29b), to compute geostophic flows.

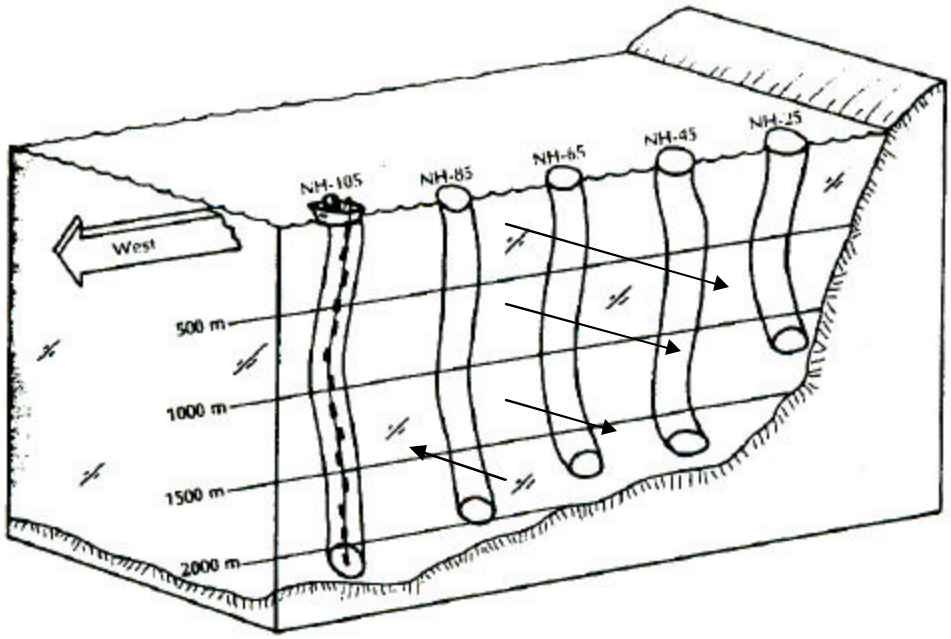

Figure 5.29b A hydrographic section off the Oregon coast. A hypothetical geostrophic flow profile is shown.

The procedure for estimating such oceanic geostrophic flow is known as the *Method of Dynamic Sections* and is based on the assumptions that ocean:

1) flow is not accelerated;
2) flow is frictionless;
3) pressure field is quasi-hydrostatic; and
4) T /S profile measurements are simultaneous (or *synoptic).*

The goal of this method is to compute the spatially-averaged geostrophic flow normal to the section between pairs of hydrographic measurement stations A and B at which hydrographic measurements were made (Figure 5.30). You will notice that the geometry of the problem is defined in terms of a quantity called *dynamic height* , which is defined as D = gz. The units of D, $\left([D] = \frac{cm^2}{sec^2} \equiv \frac{dyne\text{-}cm}{gm} \right)$ indicate that this quantity is a *work per unit mass against gravity* or a change in geopotential.

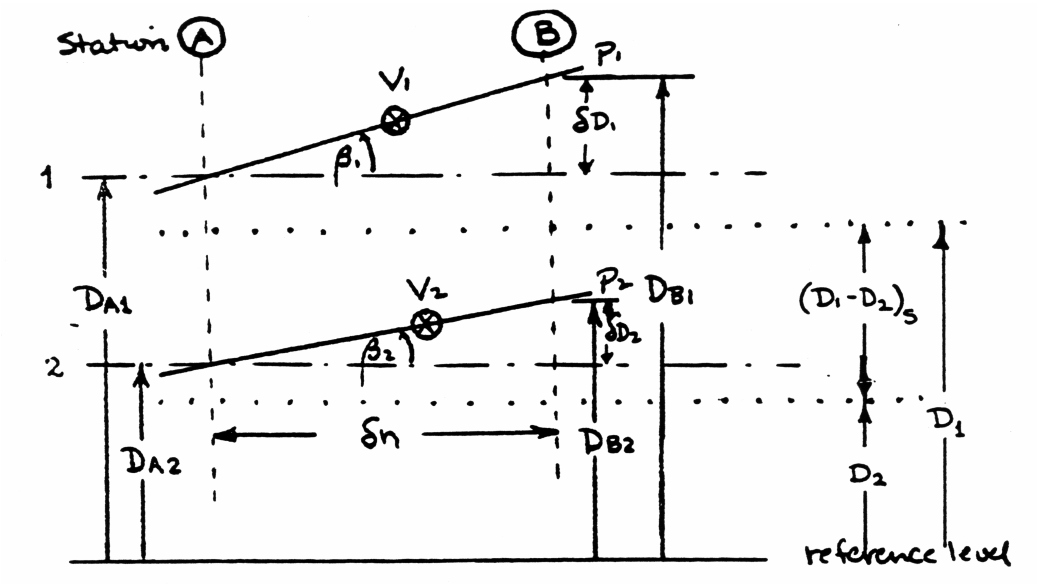

Figure 5.30 The geostrophic flow-related pressure field described in terms of dynamic heights at stations A and B. V_1 and V_2 are the geostrophic flow components normal to this plane on the respective pressure p_1 and p_2 surfaces.

More specifically, D(dynamic meter) = g z(m) ,

where g = 9.8 ms^{-2} and

$$1\ dynamic\ meter = 10^5 \bullet \frac{\text{dyne-cm}}{\text{gm}}.$$

Since $d\,p/dz = -\,r\,g$, the change in dynamic height dD = g dz can be related to specific volume according to

$$dD = gdz = -\frac{1}{r}dp = -\,a_{STP}\ dp \qquad . \qquad (1)$$

Substituting Equation (1) into the general form of the geostrophic relation

$$V = \frac{g}{f}\tan b = \frac{g}{f}\frac{\partial z}{\partial n} \qquad [or \qquad V = \frac{g}{f}\tan b \approx \frac{g}{f}\frac{d z}{d n}] \qquad (2)$$

yields

$$V = \frac{1}{f}\frac{\partial D}{\partial n} \qquad [or \qquad V \approx \frac{1}{f}\frac{d D}{d n}] \qquad (3)$$

where all the Ds are referenced to a specified geopotential within the earth. (Note that the use of dynamic height eliminates the problems introduced by the spatial changes of g).

Now apply Eq. (3) to the velocities associated with isobars p_1 and p_2, respectively (see Figure 5.30) and difference them according to

$$V_1 - V_2 = \frac{1}{f}\left(\frac{d D_1 - d D_2}{d n}\right) \qquad . \qquad (4)$$

Note that $dD_1/dn\ and\ dD_2/dn$ define the respective slopes of isobars p_1 and p_2 between observation stations A and B. Thus in terms of absolute dynamic heights, Eq. (4) becomes

$$V_1 - V_2 = \frac{1}{f\,d\,n}[(D_{B1} - D_{A1}) - (D_{B2} - D_{A2})] \quad . \tag{5a}$$

Algebraic manipulation of Eq. (5a) isolates station A and B information into separate terms according to

$$V_1 - V_2 = \frac{1}{f\,d\,n}[\underbrace{(D_{B1} - D_{B2})}_{(a)} - \underbrace{(D_{A1} - D_{A2})}_{(b)}] \quad . \tag{5b}$$

Thus the velocity of difference $V_1 - V_2$ is proportional to the difference between [term (a)] the station B dynamic height difference between intersections of isobars p_1 and p_2 and [term (b)] the corresponding station A dynamic height difference.

To compute terms (a) and (b) from observations, integrate the differential form of the dynamic height

$$dD = -\alpha_{STP}\, dp\,, \tag{6}$$

upward from D_2 to D_1 and p_2 to p_1 respectively according to ,

$$\int_{D_2}^{D_1} dD = -\int_{P_2}^{P_1} \alpha_{STP}\, dp \quad . \tag{7}$$

Evaluate the integrals in which α_{STP} has been divided into its contributions from the standard ocean and specific volume anomaly according to

$$D_1 - D_2 = [(D_1 - D_2)_s + \Delta D_{1/2}] = -\int_{P_2}^{P_1} \alpha_{35,0,P}\, dp - \int_{P_2}^{P_1} d\, dp\,. \tag{8a}$$

The left hand side of Eq. (8a) has been divided into (a) the standard ocean geopotential difference between the level isobars, $(D_1\text{-}D_2)_s$ (and thus can not contribute to any geostrophic flow) and (b) the cumulative dynamic height anomaly between isobars p_1

and $p_2\ \Delta D_{1/2}$ or

$$\Delta D_{1/2} = -\int_{p_2}^{p_1} d\ dp \quad . \tag{8b}$$

The latter contribution is responsible for the tilts in the isobars and hence the geostrophic flow departure from an exactly hydrostatic, motionless ocean.

Thus Eq. (5b) becomes the *Mohn, Sandstrom, Helland-Hansen (MSH)Relation*

$$V_1 - V_2 = \frac{1}{f\ d\ n}(\Delta D^B_{1/2} - \Delta D^A_{1/2}), \tag{9}$$

where $\Delta D_{1/2} = -\int_{p_2}^{p_1} d\ dp$.

The *MSH relation* is used to compute geostrophic velocity differences between pairs of isobaric surfaces 1 and 2, bracketed by a pair of observation stations A and B. Figure 5.31 shows graphically how the geometry of the dynamic height components is related to geostrophic flows V_1 and V_2 on their respective pressure surfaces. V_1 and V_2 are absolute geostrophic velocities relative to "level" isobar 3.?

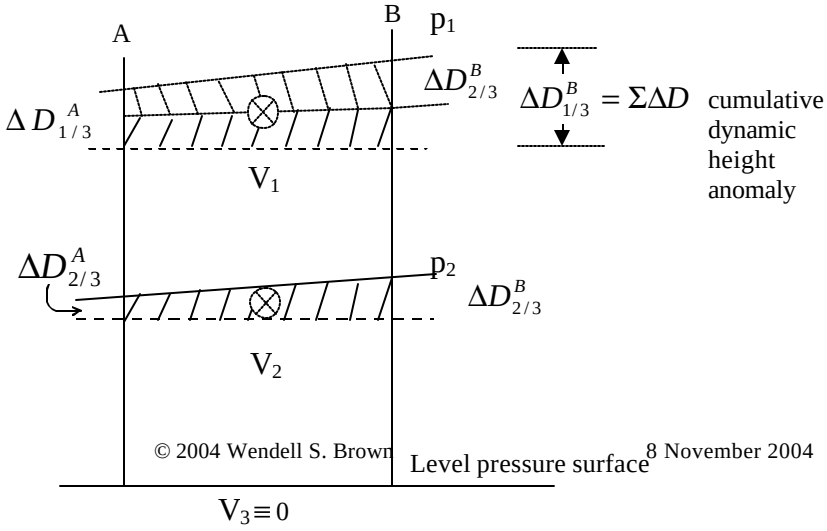

Figure 5.31 Schematic of relation of the pressure field and dynamic topography for geostrophic flow.

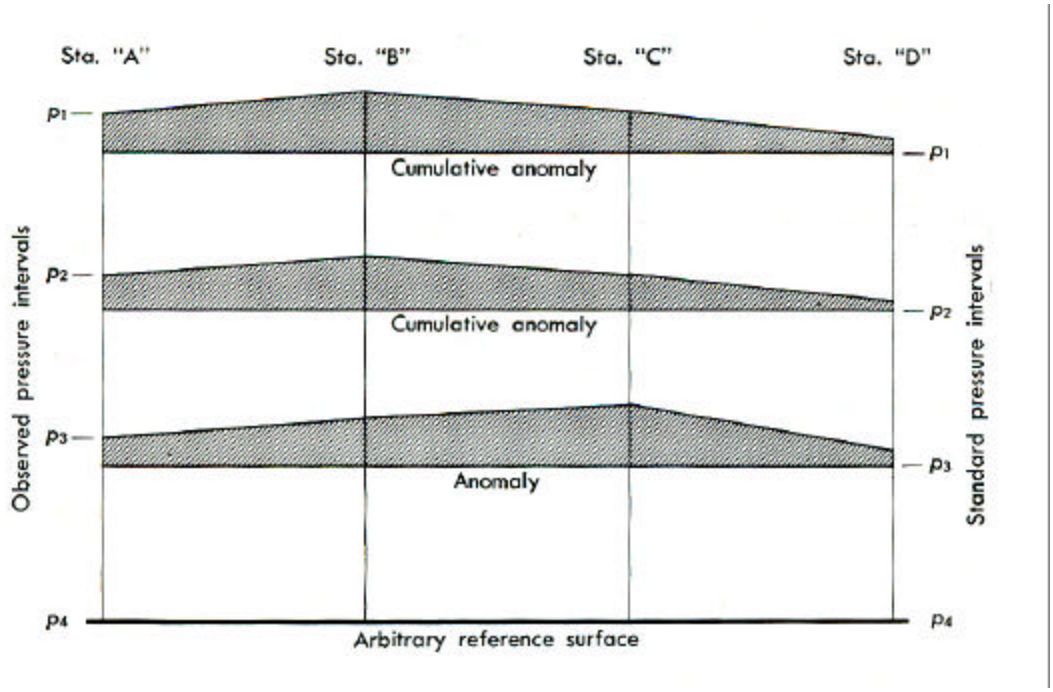

Figure 5.32 The cumulative dynamic height anomaly structure of four selected isobars (relative to the standard ocean pressure levels) for a four station hydrographic section. (Von Arx).

The schematic in Figure 5.32 graphically shows the relationship between the dynamic height, D, dynamic height anomaly, ΔD , and the cumulative dynamic height anomaly, $\sum_{n} \Delta D_n$ and the standard ocean (S = 35%, T = 0NC) pressure intervals for a realistic oceanic situation. Here we have assumed that the p_4 isobar is a level of no motion, that is, it is "level" relative to a geopotential surface and thus no geostrophic flow exists at that level.

Note that the assumption of a level of no motion permits the computation of absolute velocity at each level. Otherwise *only* relative velocity can be computed. Therefore this method is only useful in providing information about the baroclinic component of the

ocean flow. It provides *no information* about the barotropic component of the ocean flow.

An example of the application of this method to the Antarctic Circumpolar current - an essentially geostrophic current - is in Figure 5.33. (The names suggest the importance of wind forcing to the flow.) This baroclinic current is notable in that it is modest in amplitude but associated with the largest transports in the world's ocean.

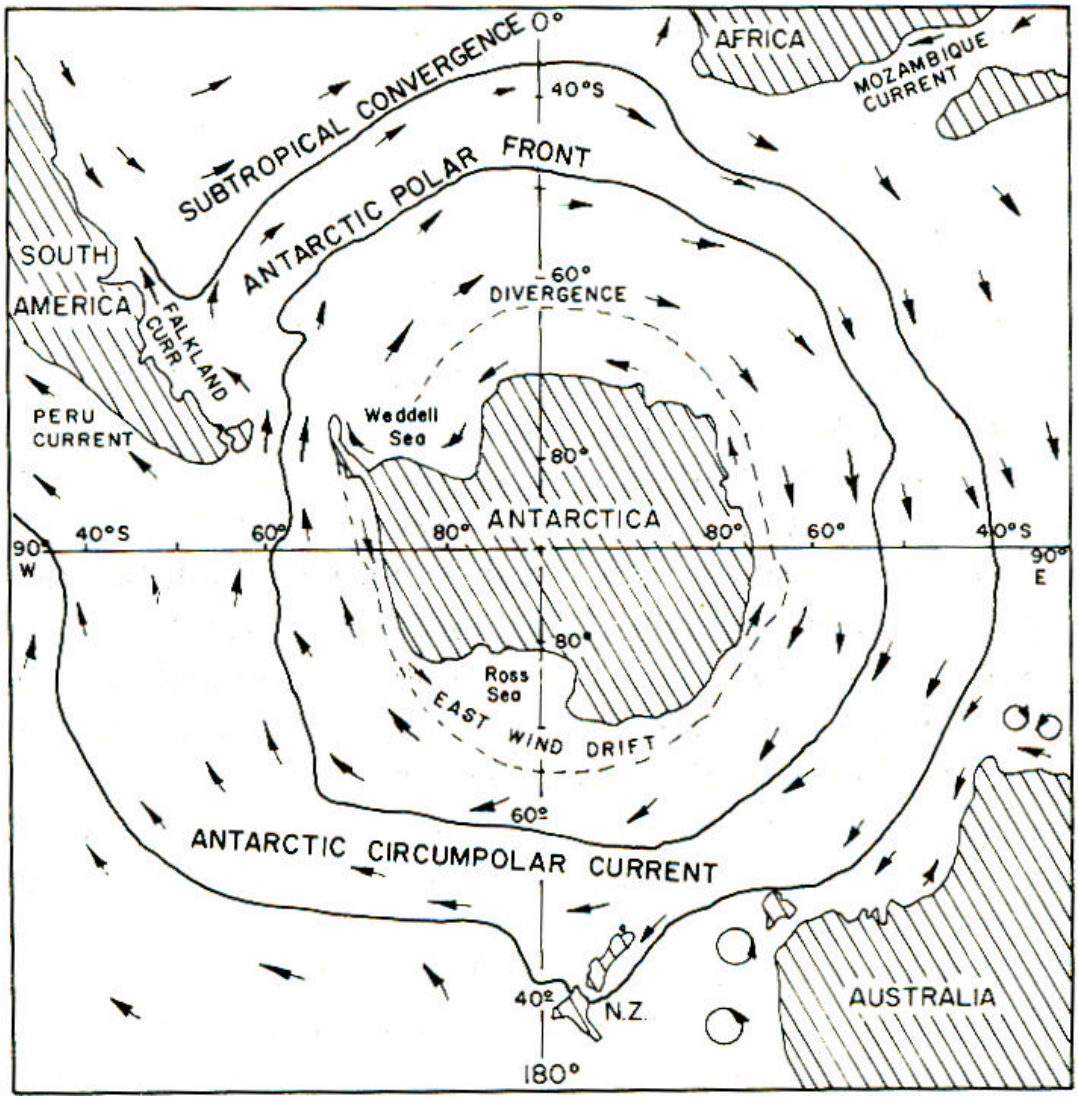

Figure 5.33. Southern Ocean surface circulation with mean positions of the Antarctic and subtropical convergences. The Cape Leeuwin, Australia, to the Antarctica hydrographic transect is indicated. (a Pickard and Emery adaptation from Deacon, "Discovery" Reports, by permission).

The lateral variation in the vertical shear in the geostrophic current is detailed in the Figure 5.34 comparison of pressure field and specific volume anomaly distributions. Note the transition from lowest flows near Australia to highest speed core in the central ocean to the more modest currents near Antarctica. Also note depth to which the currents persist.

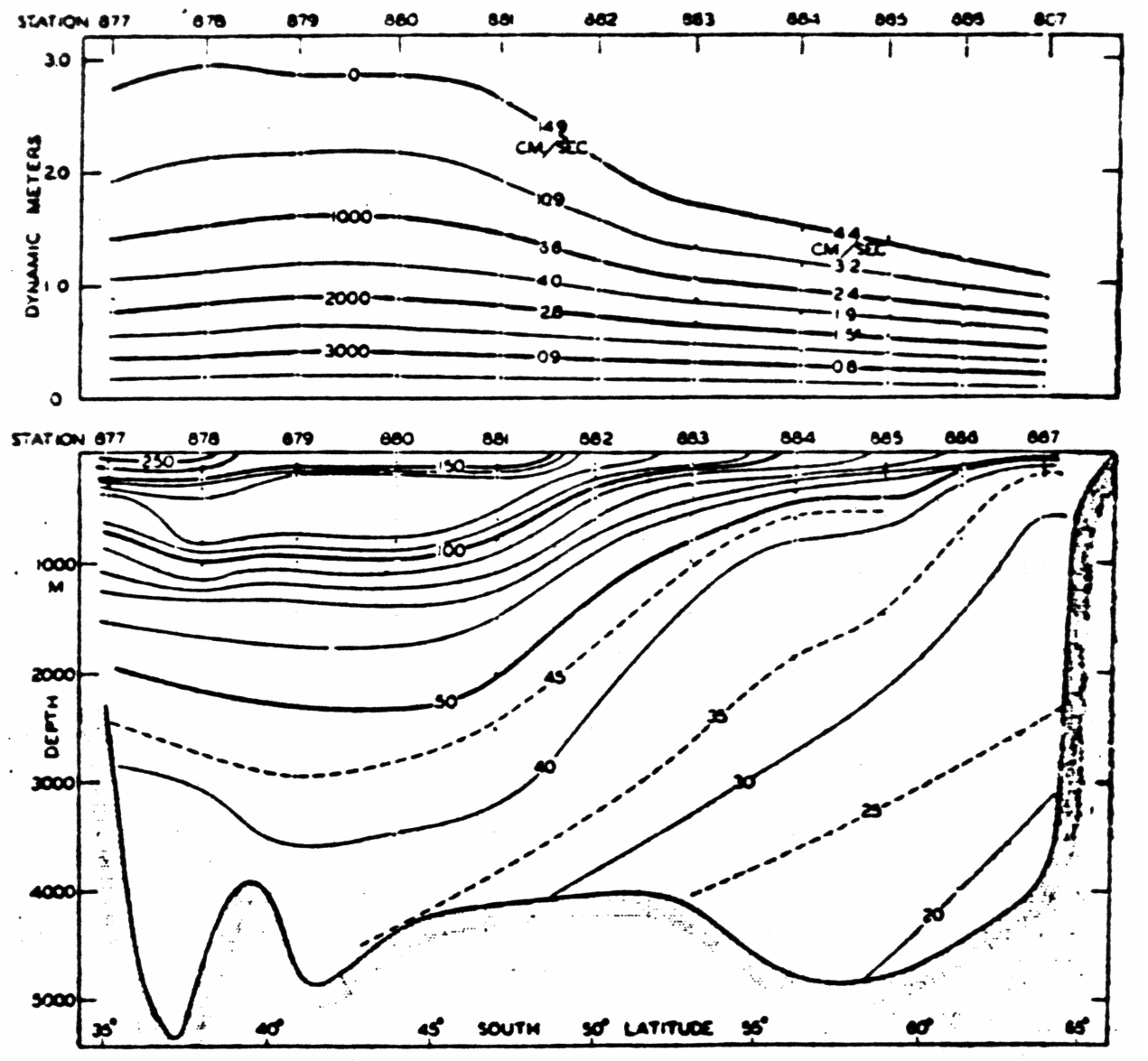

Figure 5.34 (*Lower*) Distribution of the anomaly of specific volume $10^5 d$ in a vertical section from Cape Leeuwin, Australia, to the Antarctic Continent (see Figure 5.33). *Upper:* Profiles of the isobaric surfaces relative to the 4000-decibar surface. The corresponding geostrophic velocity is indicated.

The *surface* dynamic heights of the Atlantic Ocean relative to an assumed level of no motion at 4000 db are contoured on the Figure 5.35 map. The units of the dynamic topography are in dynamic-centimeters (dyn-cm). In this case the surface dynamic topography is relative to the assumed level of no motion. (Maps of dynamic topography can be produced for mid-depth pressure surfaces as well.)

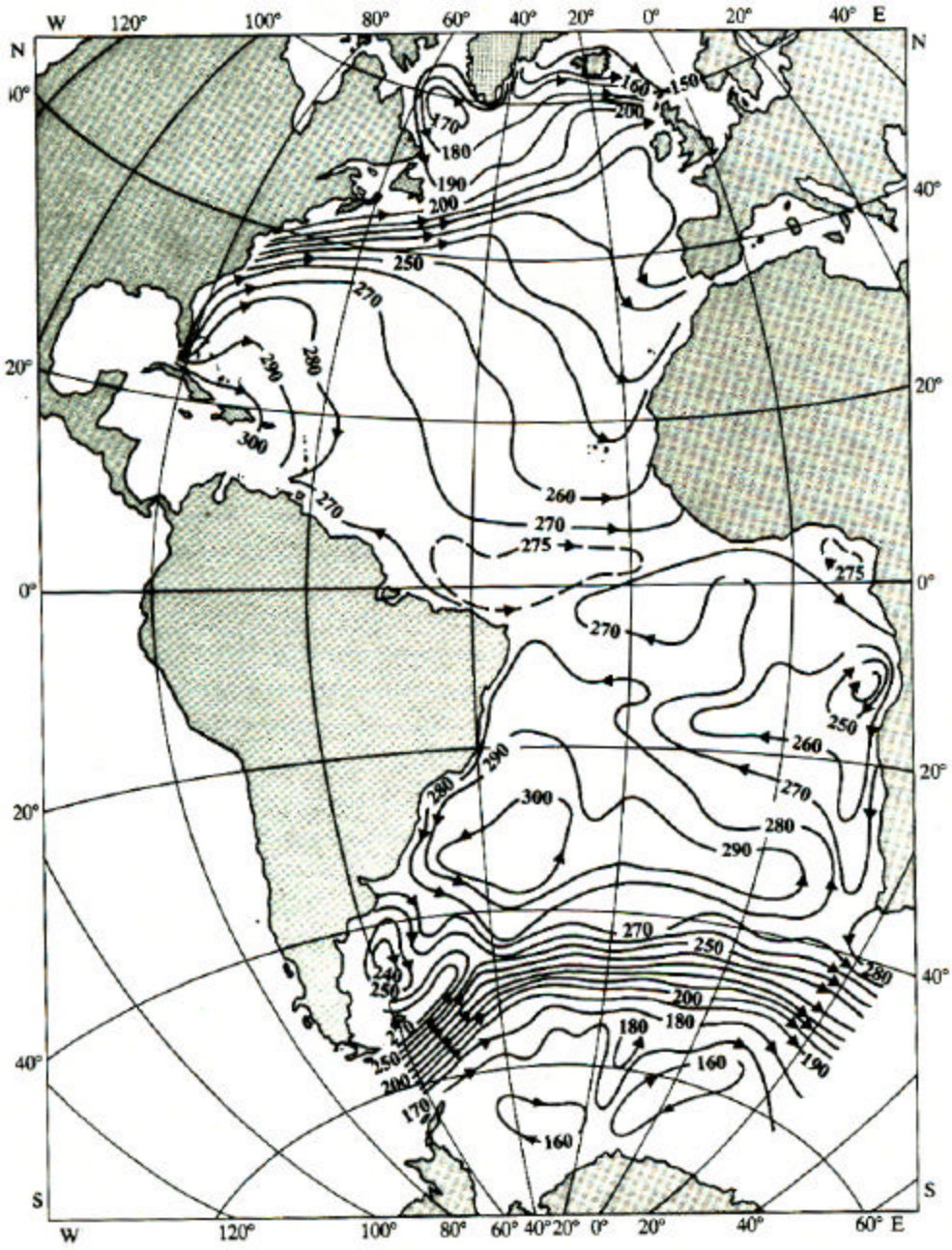

Figure 5.35 Surface dynamic topography for the Atlantic Ocean (dyn.cm rel. 4000 db) (Tolmazin).

In 1924, Wust used Gulf Stream temperature and salinity measurements (Figure 5.36a) with the Mohn, Sandstrom, Helland-Hansen relation to infer the geostrophic flow structure. The observed level of no motion was used in the Wust calculation. The similarity of the geostrophic current estimates to the direct current observations provided convincing evidence of the utility of the method of dynamic sections if a

realistic level of no motion could be determined.

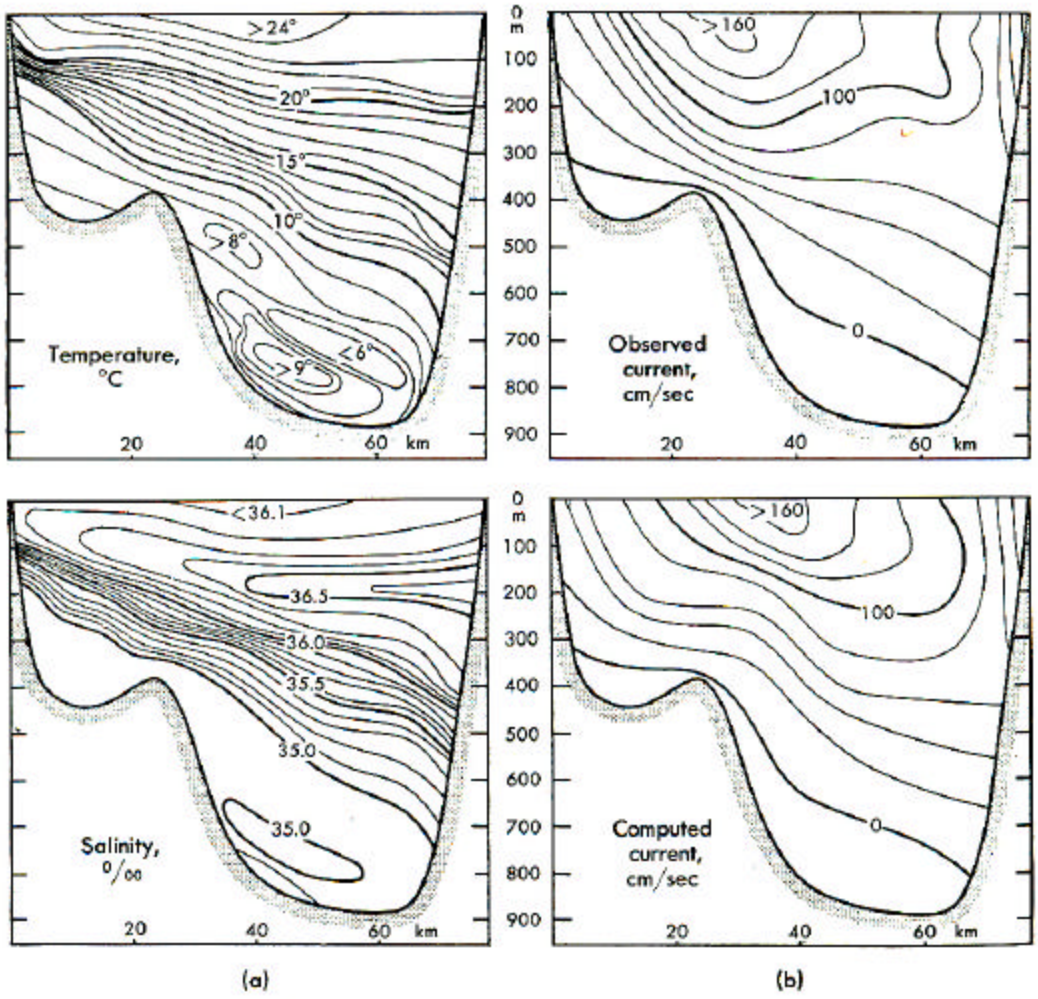

Figure 5.36a. (left) Observed temperatures and salinities in the Straits of Florida, (right) Magnitudes of the current through the straits according to direct measurements and computations on the distributions of temperature and salinity. [after Wust (19240 - From H.U. Sversdrup, M.W. Johnson, and R.H. Fleming, 1942, *The Oceans, Their Physics, Chemistry, and General Biology*, New York: Prentice-Hall.]

However until recently, simultaneous coincident current profile measurements were rare. Thus a variety of indirect methods for estimating the level of no motion have been tried over the years. For example, the surface dynamic height structure (relative to 2000db level of no motion in Figure 5.36b), based on other across-Gulf Stream T/S measurements (Iselin,1936) show where the maxima of the geostrophic surface flow of the Gulf stream would be found. Note the indication of a southward geostrophic flow (rel 2000db) east of the Gulf Stream.

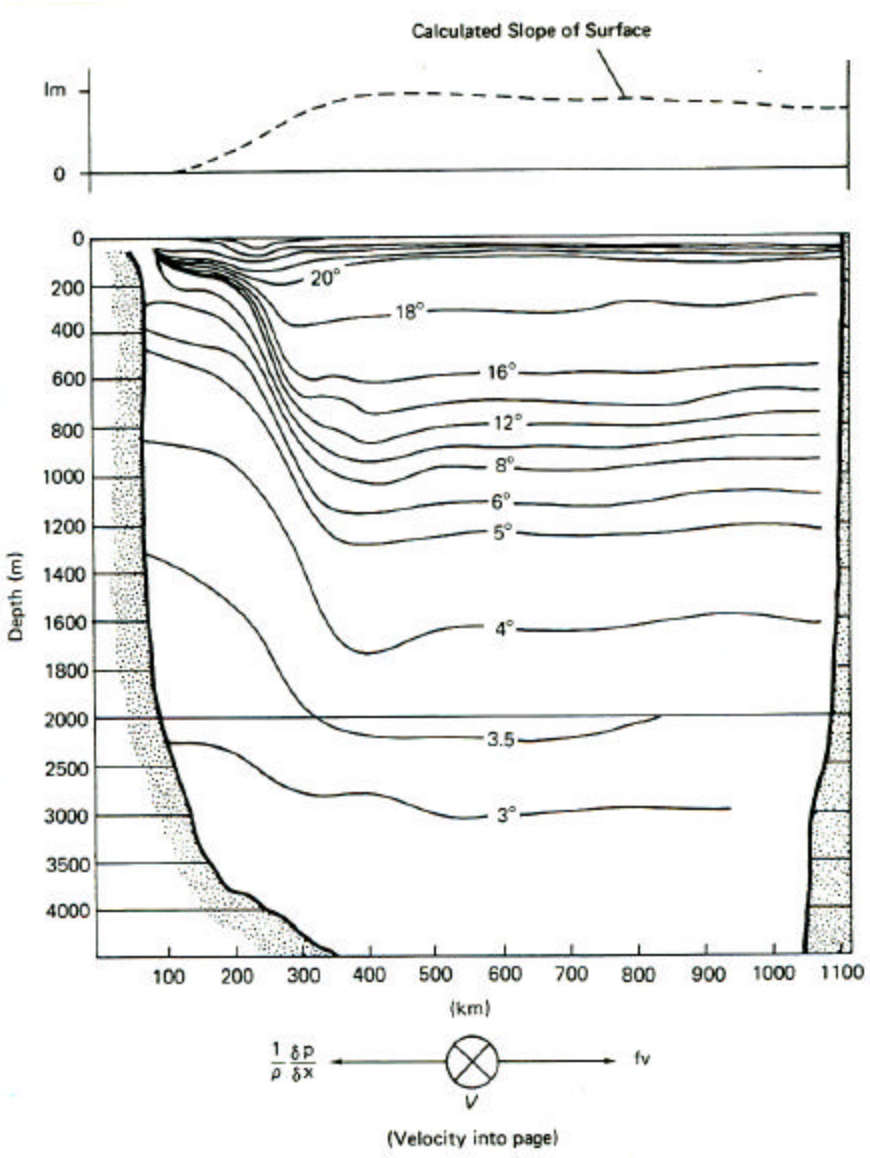

Figure 5.36b. The *surface* dynamic height determined using the MSH method and T/S measurements along of an across-Gulf Stream section from the edge of the US continental shelf on the left to Bermuda on the right. (in Knauss; after Iselin, C. O'D., 1936).

Recently oceanographers have begun estimating surface geostrophic flow from the ocean surface topography measured directly with satellite radars (see Figure 5.37). Therefore absolute deep geostrophic current structure computed using the MSH relation can now be referenced to a "known" surface geostrophic current.

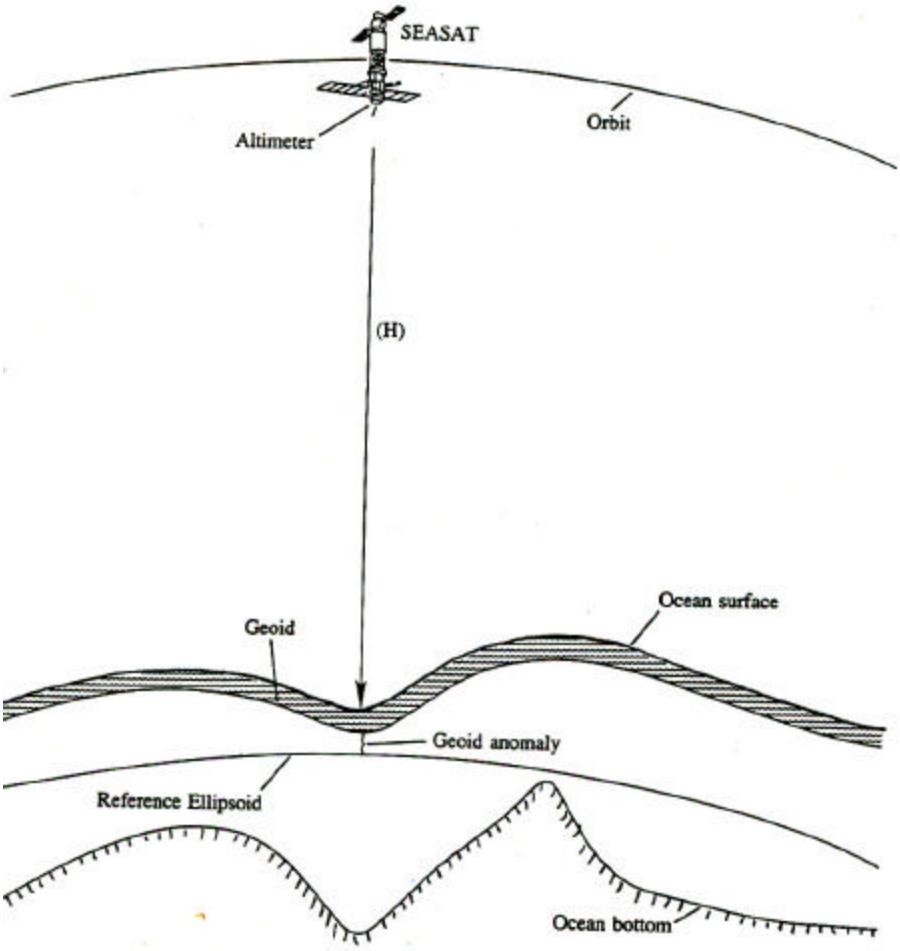

Figure 5.37 The *SEASAT* altimeter measured the distance between the satellite and the ocean surface (H). Sea level elevations/depressions relative to the geoid are typically less than ±20 cm but near western boundary currents like the Gulf Stream can be as much as 1 m.

The swiftly moving satellite uses accurate radar to measure the distance of the ocean surface (H) relative to its own position. Then departures of the ocean surface from a "known" geoid can be estimated and used to compute *surface* geostrophic flow normal to the path of the satellite track as done for a SEASAT altimeter transect across the Gulf Stream in 1978 shown in Figure 5.38. One advantage of satellite altimetry is that it produces a truly synoptic measurement along its particular track. A companion disadvantage of satellite altimetry is that its area coverage is usually limited. Nevertheless the approximately 20 days it takes for a large scale satellite survey of the world's oceans is still far faster and less expensive than a comparable ship survey (even if the latter could be done).

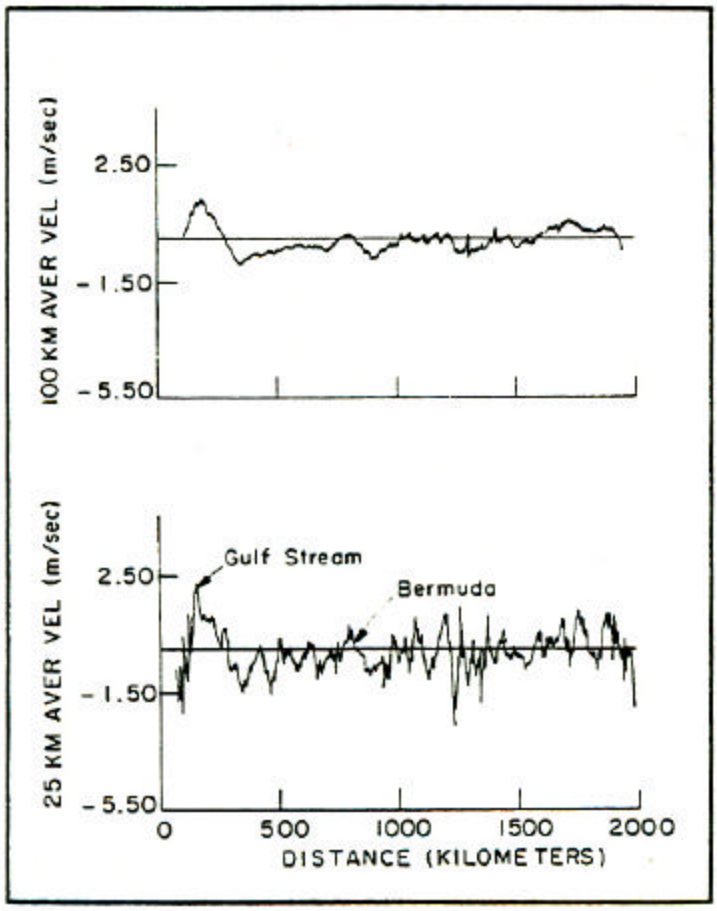

Figure 5.38 Estimates of the surface geostrophic velocity along a *SEASAT* altimetry transect crossing the Gulf Stream. The measurement noise seen in the 25km estimates in the lower panel is reduced by 100km alongtrack averging in the upper panel record. (From Wunsch and Gaposchkin, 1980).

Perhaps more importantly - absolute geostrophic flows are inferred. In contrast the shipboard method which always depends on assuming a level of no motion. The major disadvantage of the satellite altimetry is that it provides no information on subsurface geostrophic flow.

Inertial Flow – A Case of Accelerated Circular Flow

Consider the case where only the Coriolis "force" acts on a fluid parcel, with a $\vec{V} = u\,\vec{i} + v\,\vec{j}$. The component form of the momentum equation, in this case, is

$$\frac{du}{dt} = fv$$

$$\frac{dv}{dt} = -fu$$

where the flow is accelerated.

It can be shown (and you have the opportunity in Problem 5.9) that the parcel moves in a circle with a steady speed $V = \sqrt{u^2 + v^2}$. For inertial motion, the Coriolis force acts on a water parcel alone, producing a uniform circular motion*; clockwise only* in the northern hemisphere and counterclockwise in the southern hemisphere.

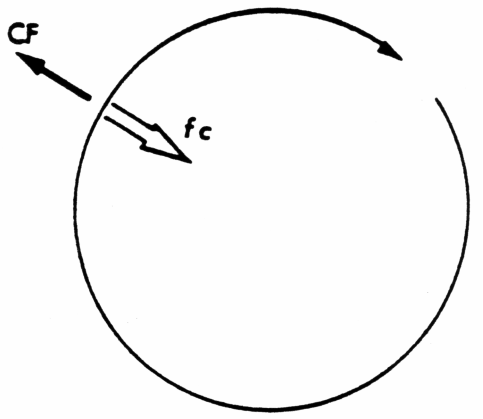

Figure 5.39a. Balance of forces for the uniform circular motion of inertial motion.

Thus the dynamics of *inertial motion* can be thought of as a dynamic balance between two pseudo-forces, namely the Coriolis force (which symbolically here is f_c) and the centrifugal force CF that is associated with the acceleration of circular motion (see (Figure 5.39a). Thus the force balance (per unit volume) for inertial motion is

$$f_c = r\,f\,V = r\,\frac{V^2}{R} = CF$$

so

$$\mathrm{f}\, V = \frac{V^2}{\mathrm{R}}$$

and the radius of the circle is

$$R = \frac{V}{f} = \frac{V}{2\Omega \sin f}$$

Here the circular water parcel trajectory has a radius R and period of the oscillation of

$$\mathrm{T} = \frac{2p\ \mathrm{R}}{V} = \frac{2p}{\mathrm{f}} = \frac{p}{\Omega \sin f} \qquad ,$$

which you will note is independent of R! The *inertial period* T is one half of a *pendulum day* which is defined as. A pendulum day is the time it takes for the vertical plane, in which a pendulum swings, to rotate $2p$ radians or 360^o relative to the earth at a particular latitude (e.g., Foucoult's pendulum).

Examples –

At the north pole $f = 90° \Rightarrow$ $\mathrm{f} = 2 \times (0.729 \times 10^{-4}\ \mathrm{s}^{-1}) \sin 90^o$

$\mathrm{f} = 1.458 \times 10^{-4}\ \mathrm{s}^{-1}$

$\mathrm{V} = 10\ \mathrm{cm\ s}^{-1}$

$$\mathrm{R} = \frac{10}{1.5 \times 10^{-4}} = 0.67 \times 10^5\ \mathrm{cm} = 0.67\ \mathrm{km}$$

$\mathrm{T} = 11.97\ \mathrm{hr}$

At $f = 30°$ $\mathrm{f} = 0.729 \times 10^{-4}\ \mathrm{s}$

$\mathrm{V} = 10\ \mathrm{cm\ s}^{-1}$

$\mathrm{R} = 1.37\ \mathrm{km}$

$\mathrm{T} = 86189\ \mathrm{s} = 23.94\ \mathrm{hr}$

$\mathrm{V} = 10^2\ \mathrm{cms}^{-1}$ $\mathrm{R} = 13.7\ \mathrm{km}$

Inertial motion is observed, particularly after the passage of storms with strong winds through a region. Beginning in the 1960s, with the development of long-term moored current measurements (Figure 5.39b), physical oceanographers have discovered strong evidence of inertial motion in current meter time series (Figure 5.39c). One method for displaying the contributions of inertial motion is to plot patterns of flow displacement past the current meter in a form called a progressive vector diagram (PVD, Figure 5.39d).

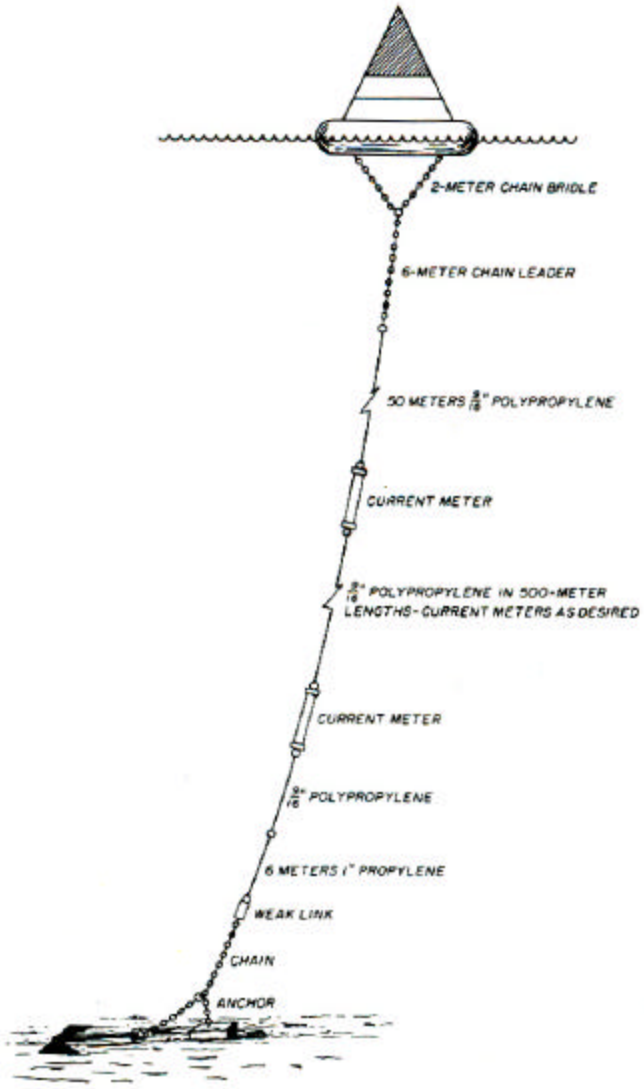

Figure 5.39b Moored array of current meters (Neumann & Pierson)

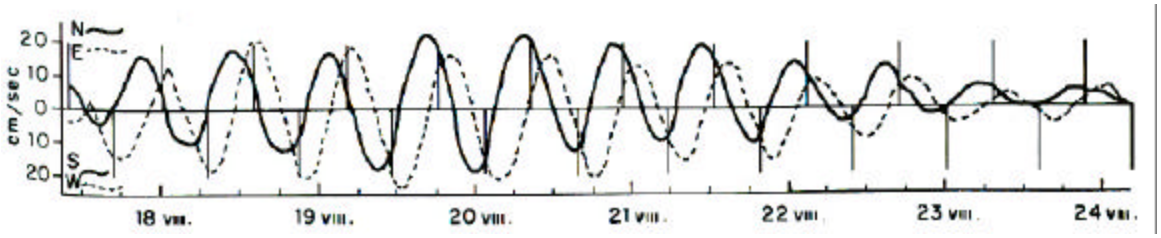

Figure 5.39c A 7-day time series of the eastward (E; dashed) and northward (N; solid) measured currents in August (VIII), indicating strong circular inertial motion. (Neumann & Pierson)

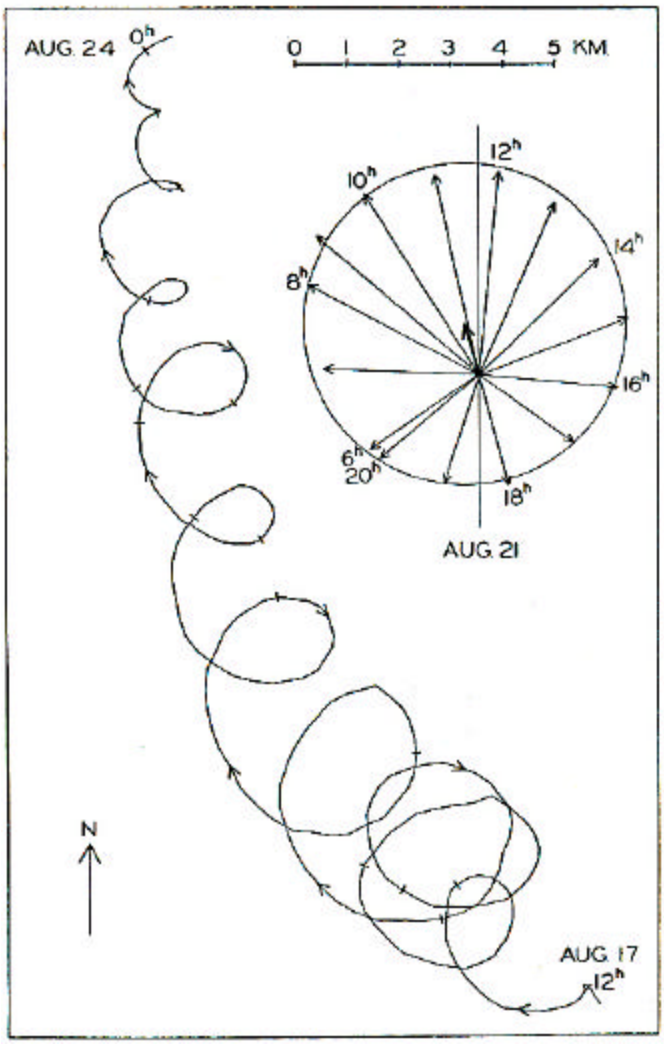

Figure 5.39d A 7-day **progressive vector diagram of moored current measurements** time series, clearly indicating strong circular inertial motion superposed on a larger scale northwestward flow. (Neumann & Pierson)

Cyclostrophic Motion: Another Case of Accelerated Flow

Consider the case of cyclostrophic motion, where earth rotation effects are unimportant and yet water parcels undergo small-scale (order 100m) uniform circular motion (accelerated - like the inertial flow case above) under the influence of *lateral pressure gradients*. The component form of the momentum equation, in which we have neglected the less important Coriolis terms, is

$$\frac{du}{dt} = -\frac{1}{r}\frac{\partial p}{\partial x}$$

$$\frac{dv}{dt} = -\frac{1}{r}\frac{\partial p}{\partial y}$$

Thus the force balance for cyclostrophic motion can be thought of as is between the centrifugal force (CF) associated with the relevant uniform rotation rate ? of the fluid and the generalized pressure gradient force ($grad_h$ p). The balance between the horizontal pressure gradient force ($grad_h$ p) and centrifugal force (CF) for rotation in either direction is:

$$grad_h\, p = \frac{\partial p}{\partial n} = \frac{\partial p}{\partial r} = r\,\frac{V_m^2}{r} = CF \qquad ,$$

where $V_m = w\,r,\ w\ is\ the\ fluid\ rotation\ rate$, and r is the radius of curvature of the flow. Thus the above becomes

$$\frac{1}{r}\frac{\partial p}{\partial n} = \frac{V_m^2}{r}$$

$$\frac{1}{r}\frac{\partial p}{\partial n} = w^2 r$$

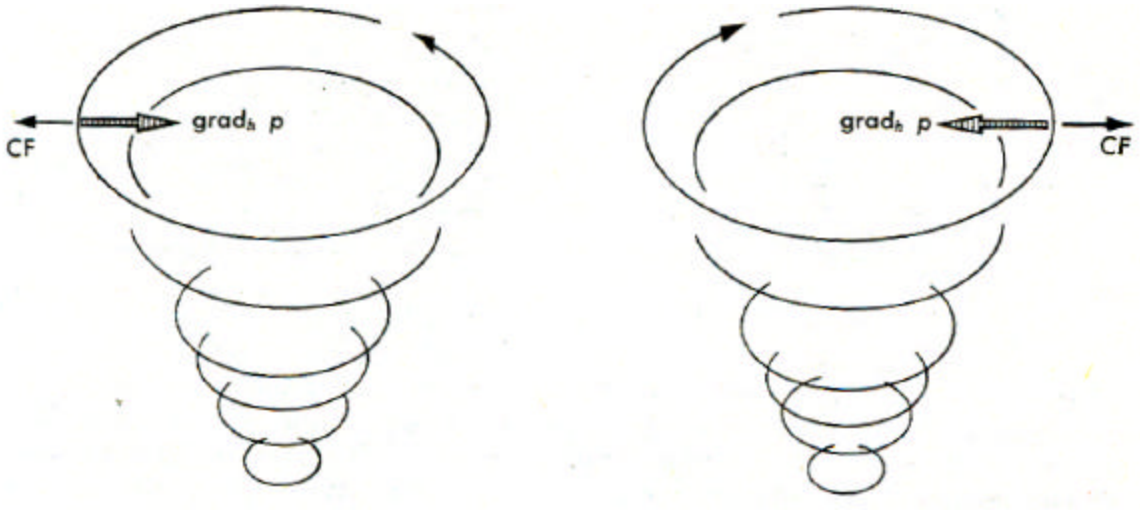

Figure 5.40 Balance of forces in cyclostrophic flow**.**

Meander Flow: Still Another Case of Accelerated Flow

Meander flow is a dynamic departure from classical geostrophic flow, in that the latter is rectilinear (i.e., straight-line flow); consistent with our original assumption of unaccelerated flow (with no curvature). There is *significant curvature* in meander flow, so the component form of the relevant momentum equation is

$$\frac{du}{dt} = fv - \frac{1}{r}\frac{\partial p}{\partial x}$$

$$\frac{dv}{dt} = -fu - \frac{1}{r}\frac{\partial p}{\partial y}$$

Thus the dynamics of meander flow can be thought of as a force balance between the lateral pressure gradient force, the Coriolis and the centrifugal force according to

$$\frac{1}{r}\frac{\partial p}{\partial n} = fV_m \pm \frac{V_m^2}{r} \quad ,$$

where r is the radius of curvature of the flow. The choice between signs depends upon the flow direction.

For *cyclonic flow* (in the sense of **f**), such as that found in a cold core ring (right Figure

5.41a), the Coriolis and centrifugal forces add (see upper right Figure 5.41b). Therefore

$$V_m = -\frac{rf}{2} \pm \sqrt{\left(\frac{rf}{2}\right)^2 + \frac{r}{r}\frac{\partial p}{\partial n}} \, .$$

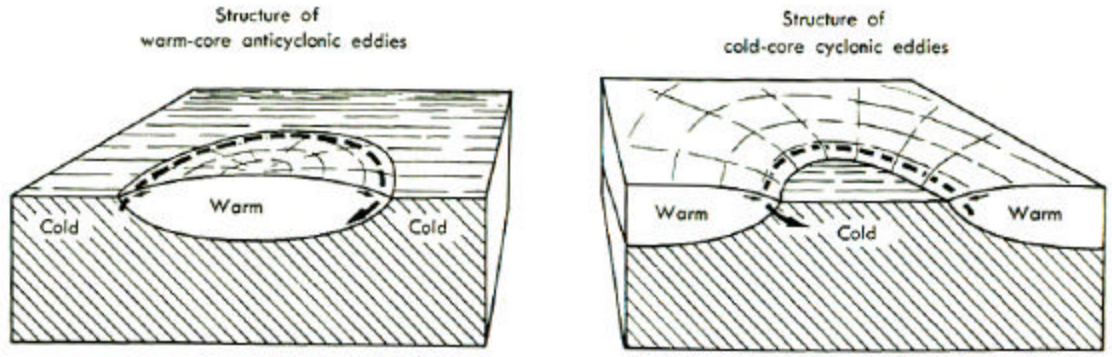

Figure 5.41a. Northern Hemisphere structure of (left) warm-core, anticyclonic eddies (right) cold core ring structure.

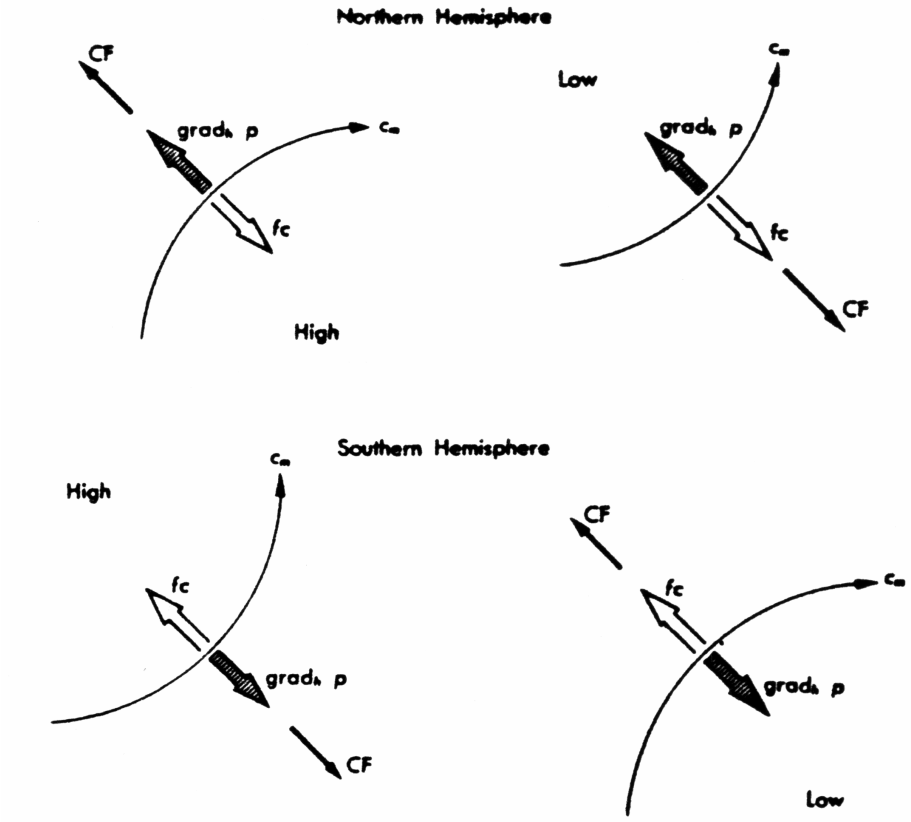

Figure 5.41b Four possible force balances for meander flow $V_m = c_m$ (Von Arx).

Since $V_m \to 0$, as $\frac{\partial p}{\partial h} \to 0$, we choose the positive solution, i.e.

$$V_m = -\frac{rf}{2} + \sqrt{\left(\frac{rf}{2}\right)^2 + \frac{r}{r}\frac{\partial p}{\partial n}}$$

For the anticyclonic flow, such as that found in a warm core ring, the centrifugal force adds to pressure gradient force. Therefore

$$V_m^2 - rf\ V_m + \frac{r}{r}\frac{\partial p}{\partial n} = 0.$$

Solving yields

$$V_m = \frac{rf}{2} + -\sqrt{\left(\frac{rf}{2}\right)^2 - \frac{r}{r}\frac{\partial p}{\partial n}}$$

As above, there is no motion for zero pressure gradient, i.e. $V_m \to 0$ as $\frac{\partial p}{\partial n} \to 0.$

Thus the minus sign is the proper one.

Presumably $$\frac{r}{r}\frac{\partial p}{\partial n} \le \frac{r^2 f^2}{4}$$

$$\frac{\partial p}{\partial n} \le \frac{r f^2 r}{4}$$

i.e. pressure gradient force < Coriolis force. In fact, for small r in atmospheric flow - pressure gradients are weak (calm conditions).

FRICTION EFFECTS

Frictional effects on ocean currents are usually confined to regions near the boundaries. The wind is coupled to the surface layer of the ocean through frictional effects in a near surface layer. Near the bottom friction slows the flow above it. In the former case momentum is added to the flow and in the latter case momentum is extracted. So it is not surprising that velocity profiles like the one in Figure 5.42 are related to stress, t.

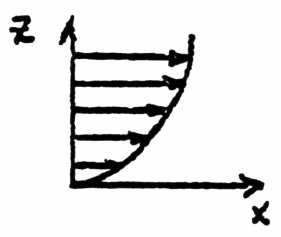

Figure 5.42. Typical boundary layer air flow near a solid (or watery) horizontal boundary.

In fact on a molecular scale x-directed horizontal stress is proportional via a coefficient of dynamic viscosity to the vertical gradient of eastward flow according to

$$t_{zx} = m \frac{\partial u}{\partial z}.$$

The units of stress are force per unit area

$$[t] = \frac{ML/T^2}{L^2}$$

which can also be expressed as a momentum flux;

$$= \frac{ML/T}{L^2 \cdot T}$$

Thus stress is this case t_{zx} is a measure of the transport of x-directed momentum in the z direction per unit area per unit time.

The *dynamic viscosity* (with units $[m] = \frac{M}{LT}$) depends upon the molecular properties of the fluid. A related quantity, known as the molecular *kinematic viscosity* n , is defined as

$$n = \frac{m}{r}$$

with units

$$[n] = [\frac{m}{r}] = \frac{L^2}{T}$$

A typical values of n for water is 0.02 cm^2/sec.

As it turns out viscous (or friction) effects that arise in the presence of *turbulent flow* are much more important than molecular viscous effects. We can explore this form of friction by first defining what is meant by turbulent flow.

First we assume that a general flow can be divided into a *mean* and *fluctuating* part. The temporal average of a time series of a current component u is $\bar{u}$ (Figure 5.43). If u is subtracted from the total velocity, then the fluctuating part, u' remains.

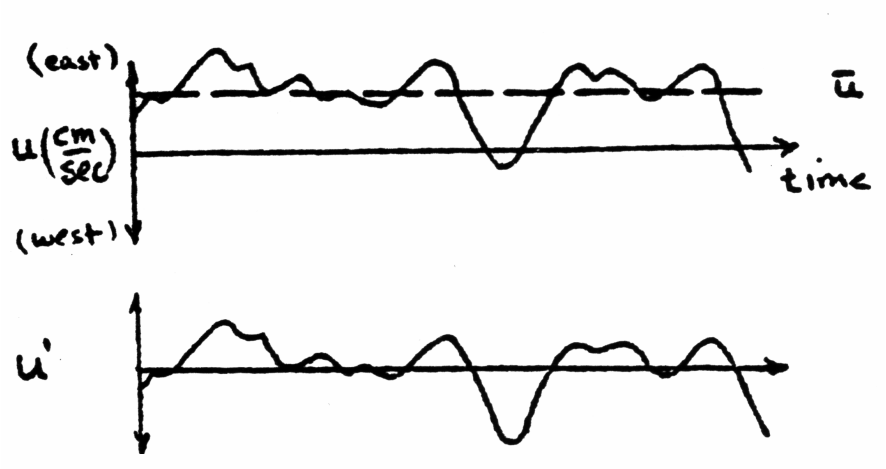

Figure 5.43. The total time-varying eastward flow **u(t)** is partitioned into its time-averaged component $\bar{u}$ and its fluctuating component u'.

Thus we can express the total velocity vector as $\vec{V} = \overline{\vec{V}} + \overrightarrow{V'}$,
where

$$\overline{\vec{V}} = \bar{u}\,\vec{i} + \bar{v}\,\vec{j} + \bar{w}\,\vec{k}$$

and

$$\overrightarrow{V'} = u'\,\vec{i} + v'\,\vec{j} + w'\,\vec{k}$$

One way of understanding how a stress arises in a flow with turbulence is to explore the momentum transport in such a flow. Given a *temporal mean* velocity profile (Figure 5.44). Consider what happens when a fluid parcel at level z_o is displaced upwards by a

velocity fluctuation + **w'** to a level $z_{1,}$ where $\overline{u}(z_1) \geq \overline{u}(z_o)$.

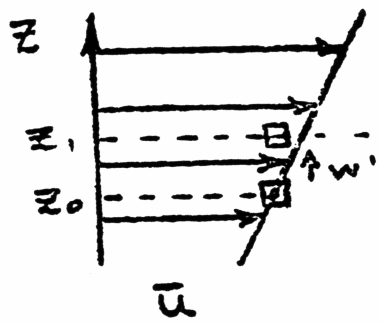

Figure 5.44. Reynolds stress in a turbulent velocity field with a mean profile as shown.

Initially at its new level, the parcel retains its original velocity $\overline{u}(z_o)$, which slower than the surrounding fluid at that level. Because the newly displaced parcel is lagging the flow at $z_{1,}$ a + x-directed **drag** force or stress is applied to the parcel until it is accelerated to the velocity of the surrounding flow. The relation of the induced drag, the + **w'** perturbation , and the horizontal velocity perturbation -u' = $\overline{u}(z_o) - \overline{u}(z_o)$ in the flow at $z_{1,}$ is shown in Figure 5.45

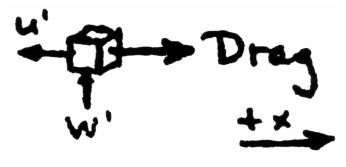

Figure 5.45. Relation of mean and turbulent flow in a shear flow.

The time average of many of these *random turbulent transport events* produces a stress S_{zx} in the fluid called the *Reynold's stress* that is given according to

$$S_{zx} = - r \overline{u'w'}$$

where the overbar ..... refers to the time-averaging process. Reynolds stress is equivalent to the turbulent flux of momentum. However it is rare that we are able to measure the turbulent velocity components. There fore, by analogy to molecular stress, we relate S_{zx} to the measurable mean velocity gradient with

$$S_{zx} = A_z^e \frac{\partial \bar{u}}{\partial z}. \qquad \text{or} \qquad S_{zx}/\rho = \nu_z^e \frac{\partial \bar{u}}{\partial z}.,$$

where A_z^e is an *eddy dynamic viscosity* and $\nu_z^e = A_z^e / \rho$ is the *eddy kinematic viscosity*. In contrast to molecular kinematic viscosity ν (which is virtually constant), ν^e *and* A^e depends upon flow conditions. Thus eddy viscosity varies in the different component directions because the flow properties vary in the different directions.

Typical values of the *vertical* kinematic eddy viscosity ν_z^e range between 2 and 10^4 cm^2/sec. Corresponding values of lateral kinematic eddy viscosity ν_H^e, (or ν_x^e and ν_y^e) are generally larger because both the "thinness" and the stratification of the ocean inhibit vertical momentum transport relative to horizontal momentum transport. Values of ν_H^e vary between 10 and 10^8 cm^2/sec.

Since eddy viscosity is so much more effective than molecular viscosity in transporting momentum (i.e. ocean frictional processes), we will use only eddy viscosities A and ν, unless stated otherwise. Although unjustified in many cases, we will further assume that the eddy coefficients A and ν are constant in space and time. In terms of this new formulation, the friction terms in the momentum equations become

x-direction $$\frac{A_h}{\rho}\left(\frac{\partial^2 u}{\partial x^2} + \frac{\partial u^2}{\partial y^2}\right) + \frac{A_z}{\rho}\left(\frac{\partial^2 u}{\partial z^2}\right)$$

y-direction $$\frac{A_h}{\rho}\left(\frac{\partial^2 v}{\partial x^2} + \frac{\partial^2 v}{\partial y^2}\right) + \frac{A_z}{\rho}\left(\frac{\partial^2 V}{\partial z^2}\right)$$

and z-direction $$\frac{A_h}{\rho}\left(\frac{\partial^2 w}{\partial x^2} + \frac{\partial^2 w}{\partial y^2}\right) + \frac{A_z}{\rho}\left(\frac{\partial^2 w}{\partial z^2}\right)$$

WIND STRESS ON THE SEA SURFACE

The winds in an *atmospheric boundary layer* are turbulent. A conceptual model of the turbulent boundary layer wind field consists of a mean wind that horizontally transports or advects an array of multi-sized eddies. The average or mean winds in this turbulent atmospheric boundary layer increase from near zero at the sea surface to its full geostrophic value at elevation as shown in Figure 5.45.

We seek to determine the horizontal stress on the sea surface t_s as a function of the wind velocity at an elevation of 15 m or W_{15}. Since the dimensions of wind stress $[t] = MLT^{-2}/L^2$, $[r] = ML^{-3}$, and $[W_{15}]$ = L/T respectively, we can surmise that

$$t = \text{const}\ r_a\ W_{15}^2 .$$

The following elaboration shows that the above "const" is 2.6×10^{-3}, so that the following empirical relation

$$t_S = 2.6\,x\,10^{-3}\ r_a\ W_{15}^2$$

for estimating sea surface wind stress with just a wind measurement at 15m elevation.

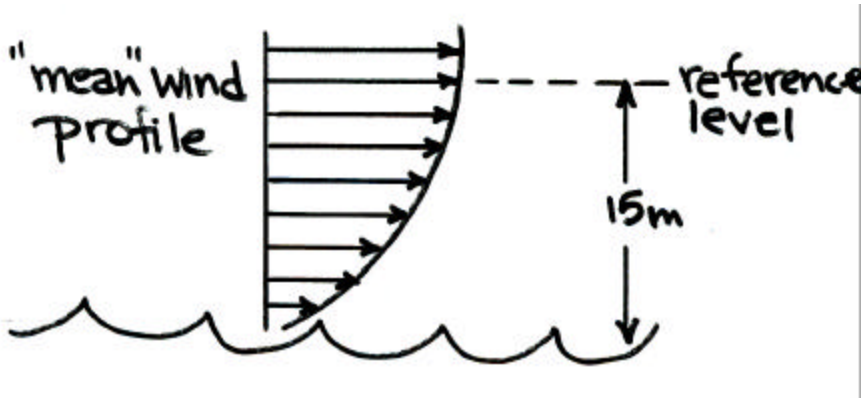

Figure 5.45 The boundary layer average or mean wind profile near an ocean/atmosphere boundary. The reference level for estimating the wind stress at the sea surface is indicated.

To derive this empirical relation for sea surface stress estimation, we *first* define a *friction velocity* u^* in terms of the stress according to

$$t_s = r_a u^{*2}$$

Second we determine u^* in terms of W_{15} as follows.

Let l be the characteristic size of these eddies, which are carried downstream at a speed u(z) that depends upon their elevation. On the other hand, these eddies can sense the changes of velocity over their own diameter, $d\,u = \frac{du}{dz}\ell$., which we assume is proportional to $\mathbf{u}^*$ according to

$$d\,u = .u*/k_o$$

where k_o is the empirically-determined "von Karmen" constant.

What length scales exist for l? The most obvious one is the height from the surface z. Therefore, if eddies have a scale z_o at the surface itself [in *this case*, $\mathbf{z_o}$ is a roughness length associated with the surface wave field, Figure 5.46], then the eddy scale at height z is

$$l = z + z_o.$$

Substituting for l and assuming that the eddy velocity $d\,u$ also scales with the friction velocity $\mathbf{u}^*$ according to

$$d\,u = \frac{d\bar{u}}{dz}(z + z_o) = \frac{u^*}{k_o}$$

or

$$\frac{d\bar{u}}{dz} = \frac{1}{k_o}\frac{u^*}{(z + z_o)} \quad ,$$

Figure 5.46. Flow eddies associated with surface roughness.

Vertical integration of the above or

$$\bar{u}(z) = \int_0^z \frac{u^*}{k_o (z' + z_o)} dz'$$

yields the mean wind profile according to

$$\bar{u}(z) = \frac{u^*}{k_o} \ln\left(\frac{z + z_o}{z_o}\right).$$

Solving the above for u^* gives

$$u^* = \frac{k_o \bar{u}}{\ln\left(\frac{z + z_o}{z_o}\right)} \quad ,$$

which upon substitution into

$$t = r_a u^{*2}$$

gives the general relation for stress

$$t_s = r_a \bar{u}^2(z) \frac{k_o^2}{\{\ln\left(\frac{z + z_o}{z_o}\right)\}^2} \quad .$$

The sea surface stress, based on the 15m mean wind $W_{15,}$ is then given by

$$t_s = r_a W_{15}^2 \frac{k_o^2}{[\ln\left(\frac{1500 + z_o}{z_o}\right)]^2}$$

Experimentally k_o and z_o are found to be 0.4 and 0.6 cm respectively, so wind stress at the sea surface is

$$t_S = 2.6\, x10^{-3}\, r_a\, W_{15}^2$$

Now we are ready to explore the effects of wind stress on the sea surface.

Ekman Flow

In 1893, Fridtjof Nansen and the R/V Fram were locked in the ice during their expedition to the Arctic. Nansen's data showed that the Fram drifted about 20° documented the to the right of the local wind direction. Upon his return in 1896, he assigned the task of deriving a theoretical explaining of this observation to a graduate student named Vagn Ekman. In 1905, Ekman published the following theory of "wind-drift" ocean currents.

The direct effects of wind stress on the sea surface are confined to a relatively thin boundary layer in the upper ocean. We can explore these effects by considering simplified versions of the horizontal momentum equations

$$\frac{du}{dt} = fv - \frac{1}{r}\frac{\partial p}{\partial x} + F_x^f$$

$$\frac{dv}{dt} = -fu - \frac{1}{r}\frac{\partial p}{\partial y} + F_y^f$$

where $F_x^f = \left(\frac{\partial t_{zx}}{\partial z} + \left[\frac{\partial t_{yx}}{\partial y}\right]\right)$; $F_y^f = \left(\frac{\partial t_{zy}}{\partial z} + \left[\frac{\partial t_{xy}}{\partial x}\right]\right)$.

First, we assume that lateral friction is negligible and that A_z and n_z are independent of z, giving

$$\frac{du}{dt} = fv + n_z\frac{\partial^2 u}{\partial z^2}$$

$$\frac{dv}{dt} = -fu + n_z\frac{\partial^2 v}{\partial z^2}$$

If we further assume that we have equilibrium flow and that the horizontal component of

$\nabla p \equiv 0$, then the force balance below results.

$$fv + n_z \frac{\partial^2 u}{\partial z^2} = 0$$

$$-fu + n_z \frac{\partial^2 v}{\partial z^2} = 0$$

The solution to these equations, assuming the application of a surface wind stress $\vec{t}_s = t_s \vec{j}$ (northward) is called *Ekman flow* or

$$u^E = V_o e^{p z/D} \cos\left(\frac{p}{4} + \frac{p z}{D}\right)$$

$$v^E = V_o e^{p z/D} \sin\left(\frac{p}{4} + \frac{p z}{D}\right) \quad ,$$

where the surface velocity $V_o \frac{t_s / r}{\sqrt{f n_z}}$ and the Ekman depth $D = p\sqrt{\frac{2n_z}{f}}$. This form (Figure 5.47) of Ekman Flow has *not* been verified experimentally. Perhaps because of our assumption that $A_z (n_z)$ is constant with depth.

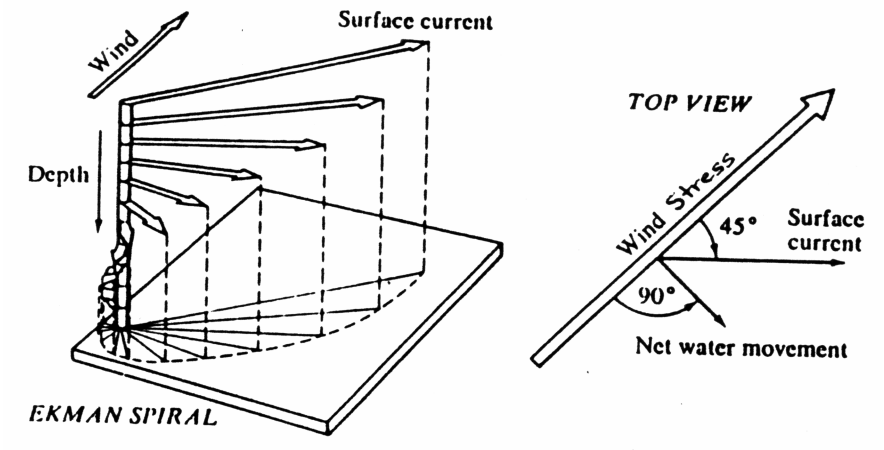

Figure 5.47 Water movements in a wind-generated current in the Northern Hemisphere.

However, if we integrate the solution above from very deep (i.e. $z = -\infty$) to the surface. We find that the Ekman Transport is

$$M_y^E = \int_{-\infty}^{0} v^E(z)\, dz = -\frac{\tau_{zx}(0)}{\rho f} \equiv 0$$

$$M_x^E = \int_{-\infty}^{0} u^E(z)\, dz = \frac{\tau_{zy}(0)}{\rho f} = \tau_s / \rho f$$

Thus the net transport in the Ekman Layer is to the right of the wind in the northern hemisphere. This result has been verified experimentally. Interestingly the Ekman transport is not dependent upon the value of the eddy coefficient of viscosity A_z.

What are typical depths of the Ekman Layer? At mid-latitudes,

$$10m<D<400m$$

$$f \_ 10^{-4}\ sec^{-1} \text{ and } 10 < \frac{A_z}{\rho} < 10^4 \frac{cm^2}{sec} \quad \text{so}$$

depending upon A_z.

The effects of Ekman transport are particularly evident along the western coasts of North American continents because they are poleward prevailing winds during certain times of the year. These poleward winds lead to offshore transport in the Ekman layer (Figure 5.48). Because of the presence of the coast this water is replaced by nutrient richer water from below the photic zone. Under the proper conditions this leads to higher biological productivity. Other oceanic and meteorological conditions at great distances from the *coastal upwelling region* can also influence the productivity of this region as we will see later.

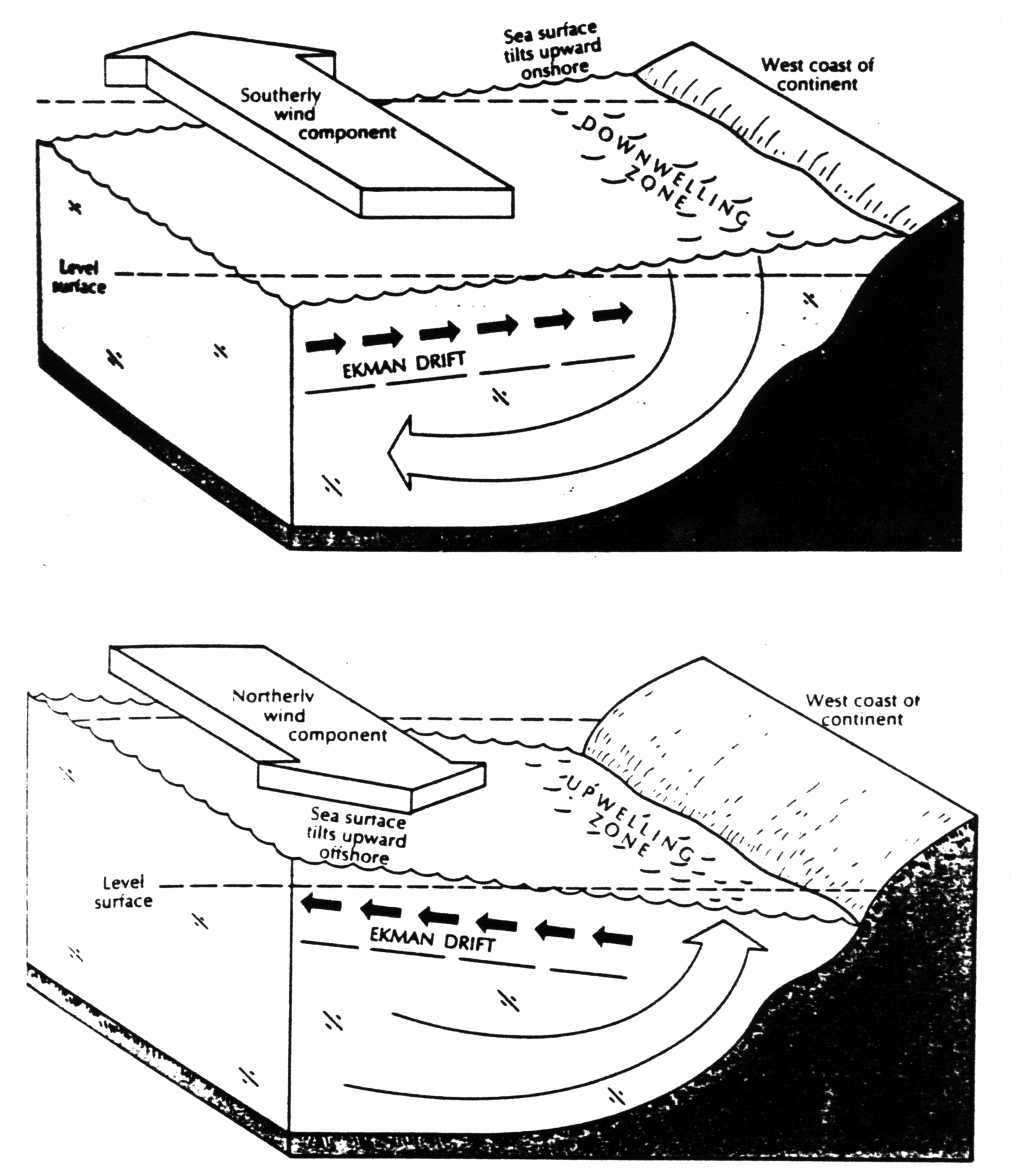

Figure 5.48. Wind-induced coastal upwelling and downwelling in the Northern Hemisphere. The slopes of the sea surface and thermocline are greatly exaggerated. The arrows show direction of water movement.

VORTICITY

In our discussions of the Coriolis "force", geostrophy, and Ekman Flow the effects of the earth's rotation on oceanic flow has been shown. This tendency of ocean flow to turn relative to an observer fixed to the earth can be discussed more clearly in terms of a quantity called *vorticity*: the tendency of water parcels to circulate around a vertical or

nearly vertical axis.

Physically, the vorticity is generally defined in terms of the *circulation* Γ (a scalar) around a line S that encloses an area A, according to the line integral

$$\Gamma = \oint_S \vec{V} \cdot d\vec{s} \quad ,$$

where $\vec{V}$ is the flow velocity and $d\vec{s}$ is the unit vector locally tangent to the enclosing line S (see Figure 5.49). The units of circulation are $[\Gamma] = L^2/T$.

Here we consider only the velocity in the horizontal plane $\vec{V}$ (x, y) so that the corresponding vertical component of the vorticity (a vector) is

$$\zeta = \frac{\Gamma}{A}$$

for which, by convention, counter-clockwise (CCW) rotation is positive upward.

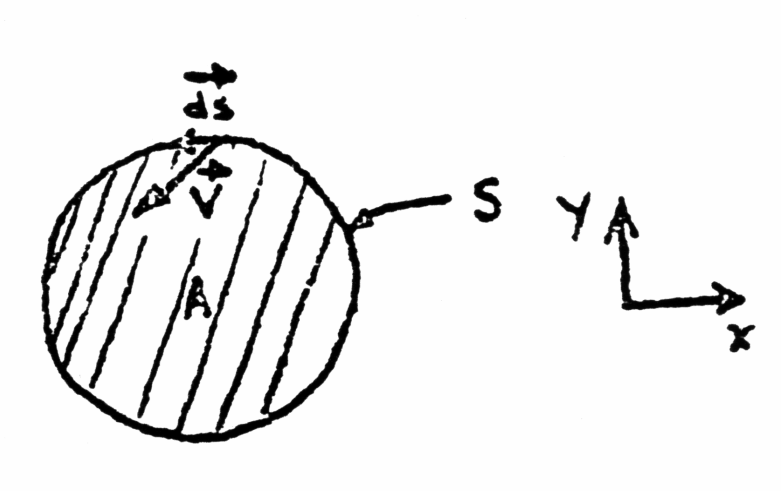

Figure 5.49 The definition of circulation in a horizontal plane.

Mathematically, the vertical component of the vorticity can be written in terms of horizontal velocity gradients according to

$$\zeta = \frac{\partial v}{\partial x} - \frac{\partial u}{\partial y} \quad .$$

This relation emphasizes the fact that flow need not be curved (or circular) in order to

have vorticity. In particular, Figure 5.50 shows the evolution of marked fluid parcel in a flow with positive shear $\partial u/\partial y$. The marking indicates that the water parcel is both advected downstream and distorted. The distortion - a *twist* – indicates that the flow field has negative vorticity or $-z$.

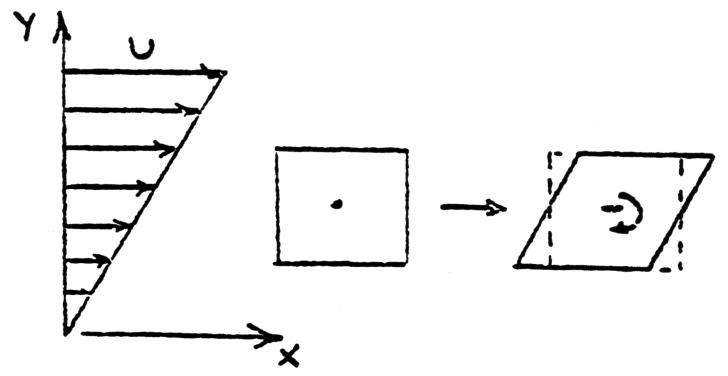

Figure 5.50 An eastward flow with northward shear advects and distorts fluid parcels, producing a combination of translation and *negative* relative vorticity.

Similarly, Figure 5.51 shows that a flow field, with a positive shear $\partial v/\partial x$, is the combination of translation and positive vorticity or $+z$.

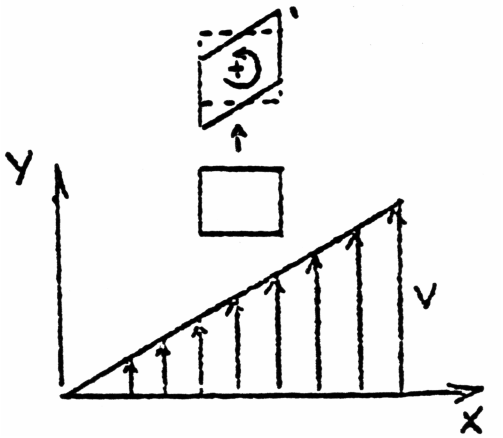

Figure 5.51 A northward flow with eastward shear advects and distorts fluid parcels, producing a combination of translation and *positive* relative vorticity.

Since vorticity is related to the rotational characteristics of the flow it is sometimes convenient to express our definition of vorticity in terms of *polar coordinates* (see Figure 5.52). Here the Cartesian x and y axes are replaced by the radial r and

azimuthal q axes. The azimuthal velocity V, which is normal (or perpendicular) to the radial (r-) direction, may vary with r - the distance from the center of curvature.

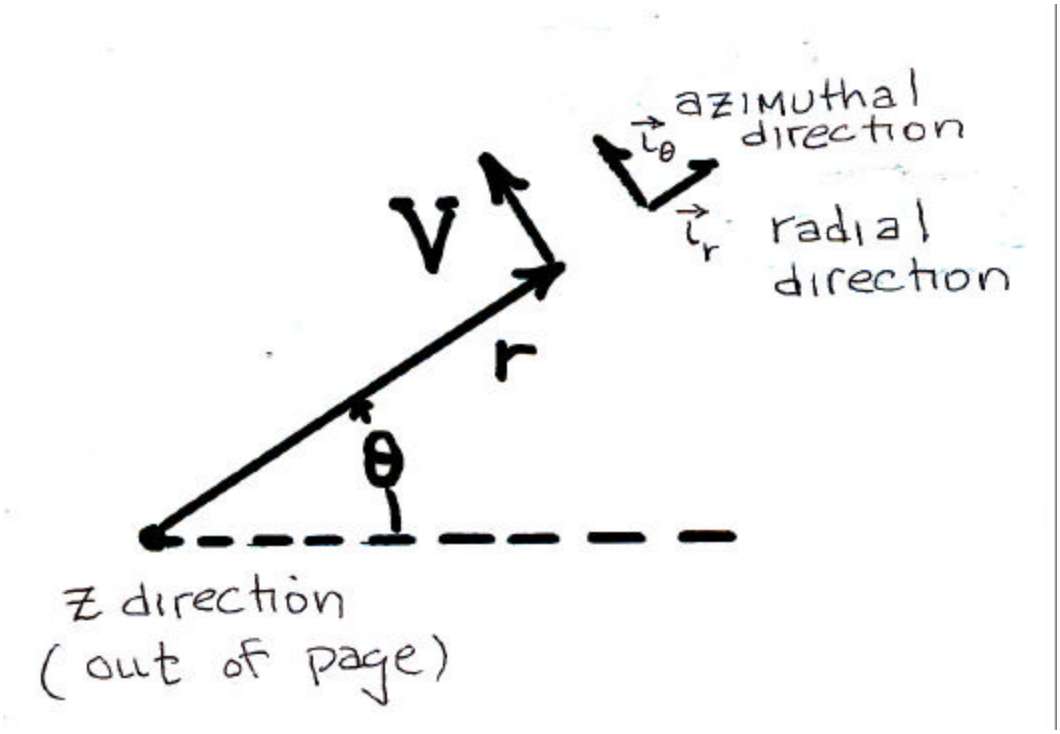

Figure 5.52 Polar coordinate system with r, q, and z coordinates in the directions of the respective unit vectors; radial $\vec{i}_r$, azimuthal $\vec{i}_q$ and upward $\vec{k}$.

In this coordinate system, the vertical vorticity - defined as

$$z = \frac{V}{r} + \frac{\partial V}{\partial r}$$

(a) (b)

has two contributions; one due to the (term a) angular velocity of the fluid as it bends through radius r; and (term b) the azimuthal current shear.

Consider the vorticity implications of the following two "flow" cases.

Irrotational Flow

The azimuthal flow in Figure 5.53a is irrotational because the "marker" lines on the

fluid parcels do not change orientation as they are advected in the flow. The vorticity for irrotational flow is zero by definition; i.e. $z \equiv 0$.

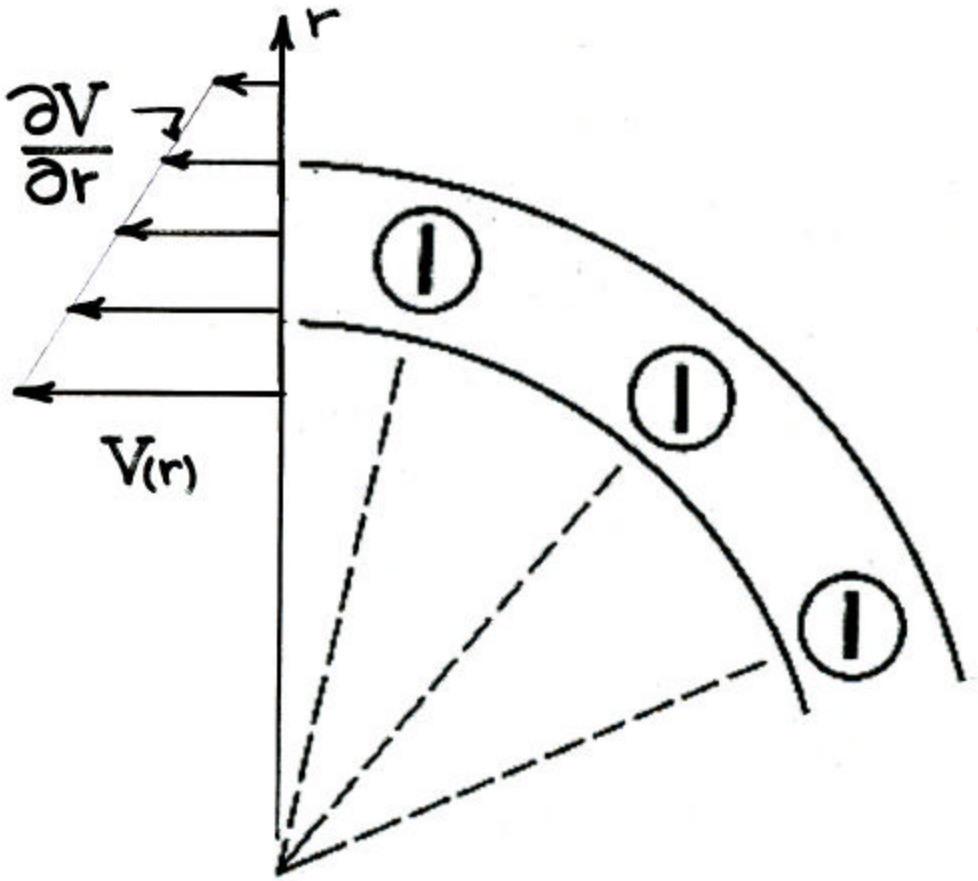

Figure 5.53a Irrotational circular flow - note the orientation of the marked fluid parcels – consists of a balance between angular velocity with a magnitude V/r and a negative shear..

Thus the two terms in the vorticity definition must balance everywhere according to

$$0 = \frac{V}{r} + \frac{\partial V}{\partial r} \quad .$$

(a) (b)

Since the curvature term (a) =V/r is positive definite, the shear term (b) must be negative. The latter means that the azimuthal velocity magnitude must decrease according to

$$\frac{\partial V}{\partial r} = -\frac{V}{r} \quad .$$

Solid Rotational Flow

Consider a resting fluid on a turntable with a rotation rate $\vec{w} = +w\vec{k}$ in Figure 5.53b. As seen by an outside observer, the fluid has a "solid body" azimuthal velocity field defined by the vector cross-product $\vec{V} = \vec{w} x \vec{r}$ (unfamiliar???; see Appendix A). The magnitude of the "flow" velocity is $V = w\,r$.

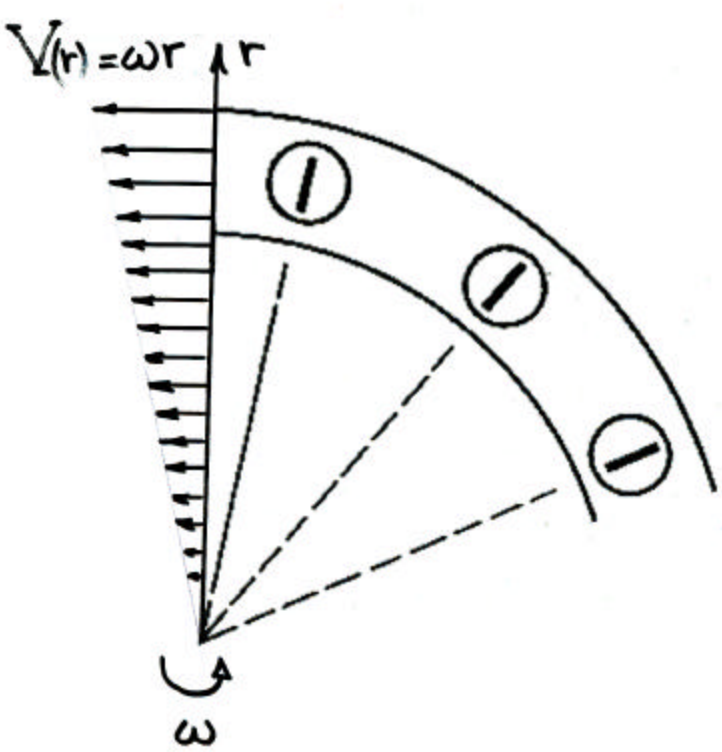

Figure 5.53b Solid-body rotary flow has an azimuthal flow magnitude $V = w\,r$. Note the

orientation of the marked fluid parcels.

What is the vertical vorticity of this flow?

Under these conditions the curvature term (a) is V/r = w ; and the shear term (b) is $\partial V/\partial r = w$; so the vorticity is

$$V = 2w \quad ;$$

or twice the angular rotation rate of the fluid.

Conservation of Oceanic Vorticity on the Earth

A *resting fluid* on the Earth will be in solid body rotation and will have a well-defined vorticity relative to an inertial frame of reference. We call this *planetary vorticity*, which is 2 times the local overhead rotation rate, or f = $2\Omega \sin f$! For example, the planetary vorticity of a fluid column at the pole is f = 2Ω ; at 30^{N}N f = O, and at the equator f = 0.

However a fluid moving relative to the Earth could have an additional component of vorticity relative to the Earth - called *relative vorticity* z . The sum of planetary and relative vorticity is called the *absolute vorticity* (AV) or

$$AV = f + z \quad ,$$

relative to an inertial frame of reference .

The ratio of absolute vorticity and the height of the water column H on a rotating Earth is called the *potential vorticity* (PV) according to

$$PV = \left(\frac{f+z}{H}\right) \quad .$$

It can be shown that under many important circumstances, the PV of a frictionless fluid column is conserved along the trajectory according to

$$\frac{d}{dt}\left(\frac{f+z}{H}\right) = 0$$

or

$$PV = \frac{f+z}{H} = cons\tan t \, .$$

Consider the implications of the conservation of PV for the following simple cases.

Case I: Figure 5.54 shows the qualitative effects of stretching and shrinking (or squashing) a frictionless water column in an f = constant environment.

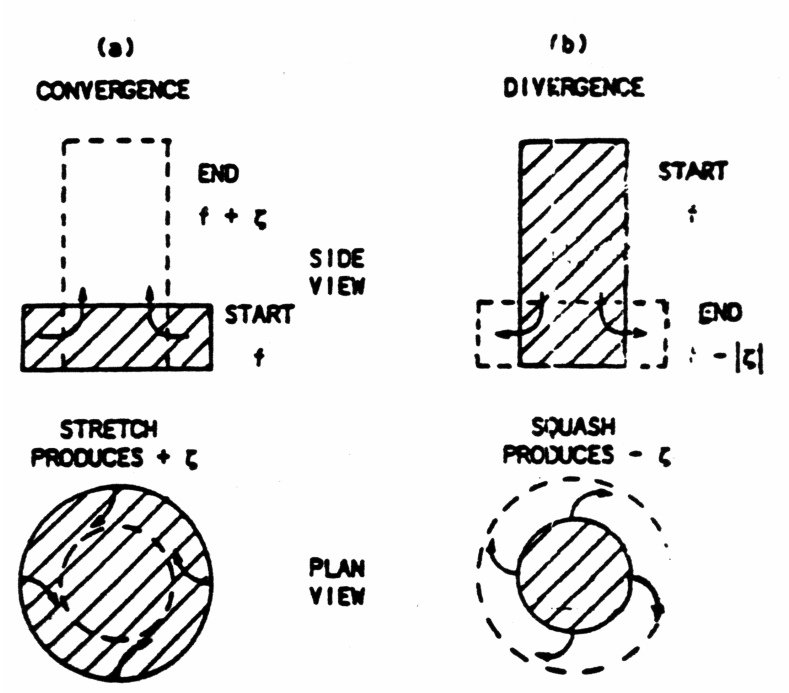

Figure 5.54. Relative vorticity change due to water column stretching.

Quantitatively (and symbolically), determine the amount and sign of the relative vorticity z that is produced, due to shrinking and/or stretching of the water column, with $f = f_o$ = a constant.

For *stretching*: Determine z after an initially motion-free ($z = 0$) fluid column is stretched to height $H_1 > H_o$, where H_o is the fluid column height at

t = 0?

To start, you know that PV conservation demands that

$$\frac{f+z}{H} = \text{constant}$$

following a water column for all time.

Thus at t = 0, the constant is

$$\text{constant} = f_o / H_o \, .$$

At some future time $t = t_1$, PV conservation demands that

$$\frac{f_o + z_1}{H_1} = f_o / H_o \, .$$

Thus

$$V_1 = f_o \left(\frac{H_1}{H_o} - 1\right)$$

For a homework exercize determine the corresponding PV change for water column shrinkage.

Case II: Figure 5.55 shows qualitatively that positive z is produced when a constant depth, frictionless water column is displaced from a poleward latitude to an equatorward latitude due to changes in f ....and visa versa.

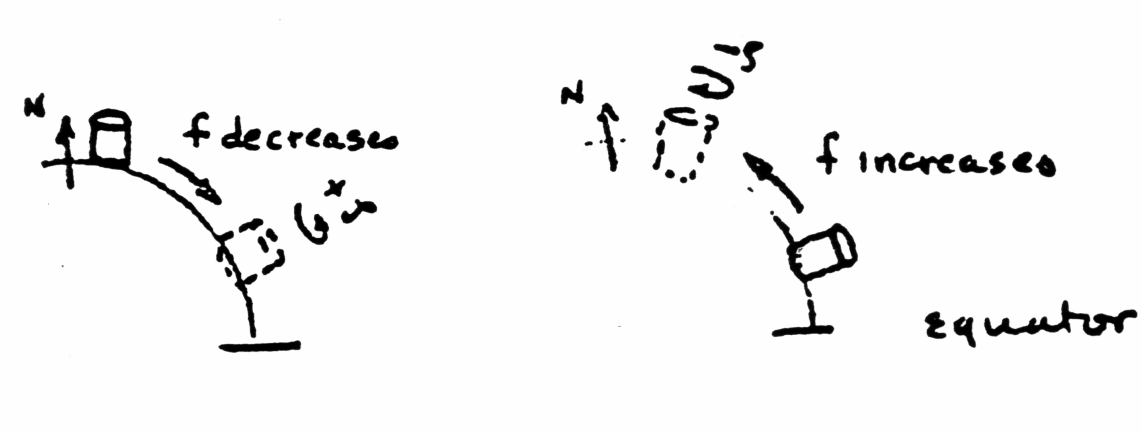

Figure 5.55 Relative vorticity change due to meridional motion.

Determine the quantitative z changes (symbolically) that are illustrated in Figure 5.55). Use the approach illustrated in the Case I analysis above.

Case III: Figure 5.56 shows qualitatively that for a situation in which changes in relative vorticity are not allowed (i.e., z production is zero), equatorward movement produces water column height H decreases and visa versa.

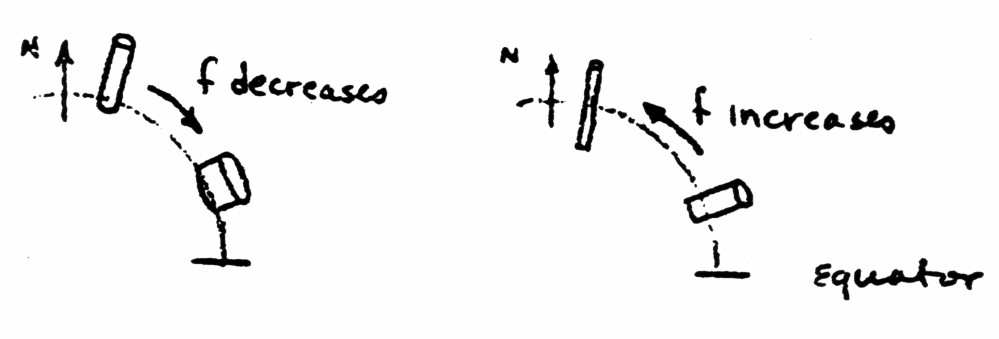

Figure 5.56 Water column stretching due to meridional motion with $\frac{dz}{dt} \equiv 0$. For zero relative

Show how PV conservation produces the z changes illustrated in Figure 5.56). Use the approach illustrated in the Cases I and II analysis above.

In this chapter, we have introduced the basic dynamic elements relevant to understanding ocean circulation. In Chapter 6, we will use many of the concepts presented in this chapter to explain the dynamics underlying wind-driven and thermohaline ocean circulation.

CHAPTER 5B PROBLEMS

Problem 5.6

Geostrophic Flow - Gulf Stream

a) The Gulf Stream flow near the surface is northward at 200 cm/sec (see diagram below).

- Assuming a latitude $\phi = 30°N$, what pressure gradient is required to geostrophically balance this flow? (recall that dimensions of pressure gradient are dynes/cm^2-cm).

- Given a 50 km-wide Gulf Stream of uniform flow, what is the pressure difference across the stream in dynes/cm^2?.....in decibars? This corresponds to how many meters (or centimeters) of excess water height?

b) Which side of the stream is higher pressure, east or west?

Problem 5.7 Water Column Dynamic Height

The diagram below shows two 2-layer water columns with different sigma-thetas. Calculate the dynamic height of the surface relative to 2000 decibars (in dynamic meters) for each water column.

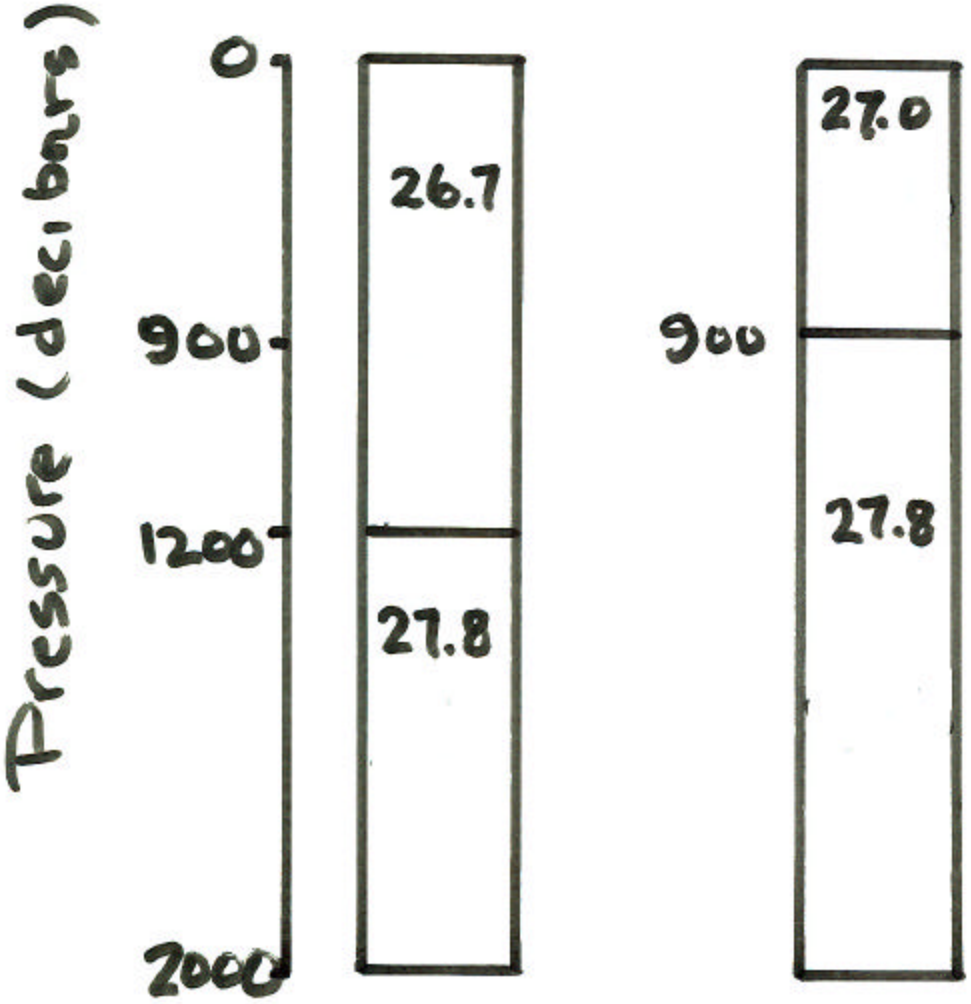

Problem 5.8 Dynamic Height Computations

You are given the following specific volume anomaly data for two stations:

Station 1	P(db) (decibars)	$d \times 10^5$ (cm^3 / gm)	Station 2	P (decibars)	$d \times 10^5$ (cm^3 / gm)
	0	350		0	650
	50	300		50	600
	100	250		100	550
	200	150		200	400
	500	100		500	200
	1000	75		1000	105
	1500	50		1500	60
	2000	40		2000	50

(a) For the two stations calculate the dynamic height anomaly difference ΔD^{p-1500} at pressures p = 0, 50, 100, 200, 500, 1000, 1500, 2000 db, according to

$$\Delta Dp^{-1500} = \int_p^{1500} d(p)\ dp$$

Hint: Try using the following trapezoidal rule approximation for an integral

$$\int_0^x f(x)\,dx = \sum_1^n \{ 1/2[f(x_1) + f(x_2)](x_2 - x_1) + 1/2[f(x_2) + f(x_3)](x_3 - x_2) + \ldots + 1/2[f(x_{n-1}) + f(x_n)](x_n - x_{n-1}) \}$$

(b) Assuming Station 2 is 100 km directly east of Station 1, and that $f = 10^{-4}$ sec^{-1}, calculate the geostrophic velocity (at each of the levels) relative to the 1500 db velocity using

$$v(p) - v(1500) = (1/f)\,d?D^{p-1500}/dx$$

What can be said about the eastward velocity component?

Problem 5.9 Dynamics of Inertial Motion

(a) Consider the movement of a solid sphere (mass = m) on a frictionless, rotating plane, with a constant Coriolis parameter = f.

If the sphere is given an initial northward velocity $\mathbf{v_o}$ at an *initial time* (**t = 0**), then at **time = t** :

- how far north has the sphere moved?
- what is the zonal (east-west) velocity?
- how far east (or west) has the sphere moved?

Hint: To answer the questions, you must set-up and solve the relevant differential equation for the motion (i.e., position, velocity and acceleration) of the sphere. To do so, consider a sphere in the figure below,with a vector $\vec{V} = u\,\vec{i} + v\,\vec{j}$ being acted upon by the Coriolis force $= \vec{F}_c = mfv\,\vec{i} - mfu\,\vec{j}$, where $u = dx/dt$ and $v = dy/dt$.

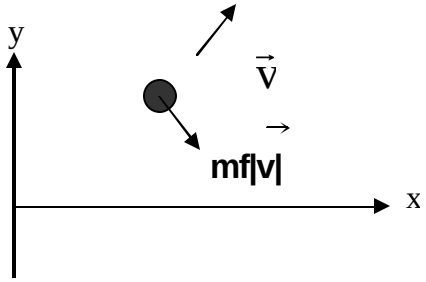

(b) Assuming an initial northward velocity of v_o = 200 cm/sec, t = 5 days, m = 1 gm, and $f = 10^{-4}$ sec^{-1}, what are the *numerical values* for the answers in part (a) ? Do your answers make sense?

(c) What are the periods (hours) and radii (meters) of the inertial circles of particles with respective speeds and latitudes of:

- 100 cm s^{-1} at 10° N latitude?
- 1 cm s^{-1} at 45° N latitude?

Problem 5.10 **Earth Rotational Effects**

Below are three different scenarios, in which earth rotation has an effect on the motion being considered. Answer the questions

A. In 1913, A.H. Compton built a large doughnut-shaped glass tube and filled it with an aqueous suspension of oil droplets to measure the local vorticity of the earth. If the contents of the tube were allowed to come to rest at latitude 30°, then

(1) What would be the angular velocity of the fluid after the glass doughnut had been very carefully overturned in its mountings?

(2) What would the angular velocity of the fluid be if the tube were quickly and carefully transported from rest at the equator to rest at the North Pole (with proper precautions having been taken to prevent freezing)?

B. For demonstration purposes, the North Pole and Southern Railway Company maintains a frictionless flat car on which is mounted a large and massive frictionless horizontal turntable. The car is frequently left on the ninetieth meridian line in the United States, for college students to push. Some students push the car northward without touching the turntable; others spin the turntable without disturbing the car. *What surprising events ensue in each case?*

C. Certain coastal regions of the earth have high biological productivity because of upwelling. If this upwelling is supported by the wind, in what direction must the prevailing winds blow on the east coasts and west coasts of the continents in the Northern and Southern Hemispheres, respectively?

Problem 5.11 **Fluid Acceleration**

A velocity field may be defined as follows:

$u(x,y,z,t) = 5t^2 + 3x + 2y$
$v(x,y,z,t) = 0$
$w(x,y,z,t) = 0$

(a) Compute an expression for the total derivative of the above velocity field. Show all work.

(b) Compute the total derivative of the velocity field at t = 2, x = 3, and y = 3. Show all work.

(c) What is the ratio of the "local" acceleration to the "advective" accelerations?

Problem 5.12 Gulf Stream Slope

A typical change in the sea surface height across the Gulf Stream is approximately 1 m. Given that the Gulf Stream is approximately 100 km in width, what is a typical sea surface slope (in degrees please!) across the Gulf Stream. Draw a diagram as part of your answer and show all work.

Problem 5.13 Pressure Gradients: Hurricane-Induced

An approaching hurricane causes a uniform, 4-m sea level rise along a north-south oriented coastline relative to a point located 100-km directly offshore at the edge of the continental shelf. Based on this information:

(a) What is the direction of the pressure gradient due to the hurricane? What is the direction of the pressure-gradient force due to the hurricane? Use a diagram and show your chosen coordinate system.

(b) What is the magnitude of the pressure gradient force caused by the hurricane "storm surge" just off the beach relative to the point located 100-km directly offshore at the edge of the continental shelf where the sea level rise due to the hurricane is 0 m? Show all work and use a diagram to help show your answer.

Problem 5.14 Pressure Gradients: Brazil Current

Given that the Brazil Current (located off the east coast of South America) has surface velocities on the order of 65 cm/s (about half that of the Gulf Stream!) and an average width of ~100 km:

(a) Estimate the magnitude and direction of the sea surface slope across the Brazil Current.

(b) Draw a diagram to help show your answer.

Problem 5.15 Ekman Flow

(a) Off the coast of Rhode Island a 4-knot wind blows from the west.

(1) What is the speed of the surface wind-generated Ekman current?

(2) To what depth does the surface Ekman current extend?

(b) Plot Ekman depth D_E versus ϕ (latitude!) from 10° N - 50° N for wind speeds of 5, 10 and 20 m s^{-1} wind speeds. Put all three plots on the same graph. What do the graphs show you?

(c) During much of the year, a steady wind blows from the south along the "scenic" northern New Jersey coast which is oriented north-south at 40° N. Assume Ekman motion and $\rho = 1.0$ g cm^{-3}.

(1) If the wind generates a surface stress of 2 dynes cm^{-2}, what is the Ekman transport along a 1-km stretch of the beach?

(2) If the average width of the continental shelf in this region is 40 km, what would be the magnitude and direction of the vertical velocity of upwelling induced by the Ekman flow over the shelf? Assume that the upwelling velocity is constant over the entire shelf.

Problem 5.16 Ocean Currents

Long-term current meter measurements located on the continental shelf south of Nova

Scotia show that average near-surface currents are westward at 20 cm/s.

(a) Calculate the alongshore (parallel to shore) and cross-shore (perpendicular to shore) components of this current taking into account the fact that the Nova Scotia coastline is oriented along a 65 degrees True compass heading. Make sure to define and sketch your coordinate systems and velocities. Show all work.

(b) A Canadian Coast Guard search and rescue team is searching for a fishing vessel which went down 100 km off the coast of Nova Scotia in the same area described above. Based on the average current velocity in the region how far along the coast and perpendicular to the coast should the search team look for survivors 24 hours after the vessel has sunk? Show all work.

Problem 5.17 Ocean Expedition Design

You are chief scientist for a physical oceanographic cruise scheduled for the month of November. A satellite-derived sea surface temperature image shows the exact location of a circular, 100-km diameter Gulf Stream warm-core ring (WCR) which has separated from the north side of the Gulf Stream south of New England. The northern edge of the WCR is located 100-km due south of Nantucket Island. Assuming you sail from Nantucket (where you maintain your own private research institution), your mission is to survey the WCR using the *R/V Sasquatch*. Your overall goal is to determine the temperature, salinity, density, and current velocity structure of the WCR relative to surrounding slope waters.

Assume the *R/V Sasquatch* can make 10 knots (cruising speed). Given what you know about WCRs, a 7-day total cruise duration, enough skilled graduate students to conduct cruise operations on a 24-hour-per-day basis, an unlimited number of XBT's (which can be deployed when cruising at 10 knots) and 3-hours for each CTD station (when stopped):

(a) Design a cruise sampling "plan" (by making an accurate sketch to scale) which will survey the WCR's surface & subsurface temperature, salinity, and density structure, the dynamic height field, and geostrophic currents measured using the "dynamic height anomaly" method described in Knauss on p. 28. Your sketch should contain the total cruise track and the locations of the WCR along with XBT and CTD station locations.

(b) Explain your sampling strategy/plan in words, discussing how you are making specific measurements, why you are making them, and any important assumptions.

(c) From your *a priori* knowledge about WCR's, what do you expect to find from your measurements?

(d) What sorts of problems should you anticipate and plan for, and how can you overcome them?

